THE 'MASSANA SOIL SYSTEM' PROJECT: UNTARGETED METABOLOMICS TO UNRAVEL CHEMICAL LANDSCAPES IN MASSANE FOREST SOILS

ALICE MARIA DE SOUZA RODRIGUES[1], MOHAMMED EL GUIF[1], ORIANE DELENA[1], JEAN ANDRE MAGDALOU[2], NABIL MAJDI[2,3], JOSEPH GARRIGUE[2], DIANE SOREL[2], ANTOINE BRIN[4], MELANIE ROY[5,6,7], DIDIER STIEN[1], EMELINE HOUËL[1*]

[1] Sorbonne Université, Université de Perpignan Via Domitia, CNRS, Laboratoire de Biodiversité et Biotechnologies Microbiennes, LBBM, 6650 Banyuls-sur-Mer, France

[2] Réserve Naturelle Nationale de la Forêt de la Massane, Argelès-sur-Mer, France

[3] Laboratoire de Recherche en Sciences Végétales, Université de Toulouse, UPS, CNRS, Castanet-Tolosan, France

[4] Université de Toulouse, Ecole d'Ingénieurs de Purpan, UMR INRAE/INPT 1201 Dynafor, Toulouse, France

[5] EDB, CNRS, Université Paul-Sabatier Toulouse III, Toulouse, France

[6] IRL IFAECI Instituto Franco-Argentino Para el Estudio del Clima y sus Impactos, CNRS, CONICET, IRD, UBA, Buenos Aires, Argentina

[7] Université du Québec en Abitibi-Témiscamingue (UQAT), Rouyn-Noranda, Canada

**Corresponding author: houel@obs-banyuls.fr*

KEYS WORDS.- OLD-GROWTH FOREST, BEECH (*FAGUS SYLVATICA* L.), UHPLC-HRMS/MS, MOLECULAR NETWORKS, PLANT-MICROBE-SOIL INTERACTIONS, CHEMICAL ECOLOGY, HETEROGENEITY, MAPPING

ABSTRACT.- Advancements in soil analytical techniques offer new insights into ecosystem structure, functions, and dynamics. Metabolomics has the potential to serve as a unique and efficient way to characterize the soil "chemical landscape." Thirty-three soil samples were collected from the Massane old-growth forest reserve, a UNESCO world heritage site located in the Eastern piedmont of the French Pyrenees. The study sites aimed to investigate three types of forest stands, namely beech forests, beech/oak stands, and mixed forest stands, subsets being also defined within stand types based on forest facies. We hypothesized that soil chemical heterogeneity would reflect forest spatial heterogeneity. Non-targeted metabolomics using liquid chromatography coupled with high-resolution tandem mass spectrometry (UHPLC-HRMS/MS) and molecular network analyses were employed to map the chemical diversity across the sampled sites. This approach unveiled the presence of various compounds, including lipids (fatty acids and their derivatives, sphingolipids, prenol lipids, steroids), terpenoids (triterpenoids and sesquiterpenes), coumarins, and oligopeptides and lipopeptides. Along with the presence of a rich core metabolome, some heterogeneity was also underscored, suggesting unique chemical structures associated with specific types of sampling sites, notably mature beech stands. These results call for a deeper investigation into these specific compounds, with regards to their biological origin and the diversity and heterogeneity of soil microbial communities.

INTRODUCTION

Old-growth forests are defined as both ancient and mature settlements, *i.e.*, that have been continuously wooded for a long period of time, and that host both many large or old living trees and large volumes of deadwood (Cateau *et al.* 2015). These ecosystems are of particular interest due to their high biodiversity, in terms of tree species and tree micro-habitats, as well as below-ground fungal or bacterial species (Larrieu & Gonin 2008, Mennicken *et al*. 2020). These biomes are typically marked by high spatial aboveground and belowground heterogeneity, making them valuable exploration fields for the development of innovative tools trying to capture variability in spatial patterns, in relation to ecological features and processes (Baldrian 2017).

Heterogeneity is notably a keystone concept in landscape ecology (Wu 2013). In this field of science, landscapes are defined as spatially diverse areas consisting of interacting ecosystems, with their analysis focusing on the interdisciplinary and dynamic examination of ecological biotic and abiotic processes (Delcourt & Delcourt 1988, Risser 1987, Van Eetvelde & Aagaard Christensen 2023). Landscapes can thus be contemplated from an integrative perspective through three main dimensions, *i.e.*, structure, function and changes, to encompass the complex interactions between mosaic elements and properties at various spatial-temporal scales (Forman & Godron 1986). Among the current challenges faced by this socio-ecological research field are the necessity to improve the design of metrics, and to design ecologically sound analytical methods that reflect the inherent heterogeneity to detect, monitor, and predict landscape changes (Wu 2013, Wu & Hobbs 2002).

In the specific context of the forest environment, spatial heterogeneity is primarily linked to tree dominance and the identity of tree species, which affects both microbial activity and the composition of microbial communities, notably fungal communities, in the soil and litter (Bahnmann *et al.* 2018, Baldrian 2017, Tedersoo *et al.* 2016, Urbanová *et al.* 2015). Tree communities have also been demonstrated to influence soil microbial resistance and resilience to drought stress in experimental plots, measured through microbial biomass, with a strong effect of tree species identity (Rivest *et al.* 2015). Complementarily, a study of tree species mixing in a set of European mature forests from different climate zones suggested an indirect influence of the composition of tree community on soil microbial parameters through the associated forest floor litter as well as absorptive root traits (Gillespie *et al.* 2021). Past landscape structure, in terms of the total area of ancient forests, has also been shown to correlate with fungal species richness (Mennicken *et al.* 2020). Plant traits and communities, soil properties, and microbial activity and communities, are thus closely interlinked, and these interactions have significant implications for the overall functioning of below- and aboveground ecosystems (Wardle *et al.* 2004). The role of plant communities in shaping the soil microbiome, and the nature and dynamics of interactions at a local scale, are thus gaining attention with respect to environmental factors (Baldrian 2017, Fierer 2017).

Overall, these intricate interactions between plants, microbial communities and soil revolve around the basal concept of metabolite production. These compounds play a crucial role in the functioning of ecosystems, particularly soil, by mediating dialogue between plants and soil microorganisms (Bonfante & Genre 2015, Mithöfer & Boland 2016, Tyc *et al.* 2017). Their key role in this tripartite relationship is increasingly highlighted in the context of plant-soil feedback processes (Delory *et al.* 2024, Semchenko *et al.* 2022), and has been especially studied for litter decomposition and the release of root exudates (Chomel *et al.* 2016, Hu *et al.* 2018). In this context, analytical studies based on metabolomics open original perspectives in ecology. Metabolomics represents the thorough exploration of a large number of low-molecular-weight compounds in a biological sample. It is widely acknowledged as the -omics discipline that most accurately reflects the phenotype (Fiehn 2002, Patti *et al.* 2012). Specifically, untargeted metabolomics, which explore global metabolite profiles, emerges as a powerful tool for gaining insights into the dynamic functioning of ecosystems by considering the metabolome as a novel functional trait (Walker *et al.* 2022). These approaches have recently been developed to investigate various aspects of plant-microbial-soil interactions in the rhizosphere (Hildebrand *et al.* 2023, Mhlongo *et al*. 2018), the impact of plant host-fungus interaction on soil metabolite profiles (Wong-Bajracharya *et al.* 2020), or the assessment of soil quality and microbial function (Withers *et al.* 2020). Notably, a recent greenhouse experiment highlighted a correlation between the metabolome of root tissue and the chemical composition of the rhizosphere in distinct *Populus angustifolia* populations, thereby establishing for the first time a link between soil chemistry and plant populations collected across different environmental gradients (Mueller *et al.* 2020). Complementary, the link between the metabolome of plant aerial parts and their environment was shown based on the combination between metabolomic studies and machine learning-based predictions (Dussarrat *et al.* 2022).

Building upon these foundations, we chose to focus on the Massane Forest National Nature Reserve to develop this study. This old-growth forest, located on the edge of the Eastern Pyrenees in southern France, is considered a relic from a Holocene glacial refuge for European beech (*Fagus sylvatica* L., Fagaceae). European beech is a keystone species of these ancient and mature forests across the European continent, and the Massane forest represents the southern limit of the *F. sylvatica* distribution area (Magri 2008). This biodiversity hotspot has been free from extensive human impacts for the past 150 years, providing a rare opportunity to study soil chemical landscape with regards to plant-microbial-soil interactions in a remarkably preserved environment (Majdi *et al.* 2024). The aim of this study was to explore the chemical landscape of various forest stands and facies. Using an approach inspired from landscape ecology, we compared the "spatially diverse areas consisting of interacting ecosystems" presented above in terms of both forest structure and metabolome. Built upon the development of analytical tools based on UHPLC/HRMS-MS untargeted metabolomic analysis and molecular networking, our hypothesis posited that the chemical heterogeneity in soil composition would reflect the spatial heterogeneity of forest landscapes mosaic.

MATERIALS AND METHODS

Study site

The sampling sites were selected in the Massane Forest National Nature Reserve (RNNM), located in Argelès-sur-Mer in southern France, at the base of the Eastern Pyrenees, approximately 5 km from the Mediterranean Sea (42°28′41″N, 3°1′26″E), between 600 and

1200 m in altitude (Fig. 1). The climate is meso-Mediterranean (Oddou-Muratorio *et al.* 2021). A mean annual temperature of 12.1 °C was measured between 1976 and 2022, and a mean annual rainfall of 1154.2 mm between 1960 and 2022. The area is exposed to important wind phenomena, notably in winter, due to the occurrence of the Tramontane North-West wind in this Mediterranean region (Obermann *et al.* 2018). The protected area, which covers 336 ha and includes the source and the upper valley of the Massane River, was created in 1973. The beech old-growth forest located within the RNNM was granted a UNESCO World Heritage Site designation in July 2021. No logging activity has taken place in the reserve since at least since 1886, and both economic exploitation, recreational camping or bivouacking, and all forms of sampling are now strictly prohibited all over the RNNM area. Additionally, since 1956, a 10-ha fenced plot has been established as an historical core reservation zone, serving the purpose of preventing cow grazing in this sector (Delamare Deboutteville *et al.* 1957). The beech old-growth forest accounts for over 50 % of the reserve area, alongside semi-natural grassland habitats on the ridge of the perimeter. Depending on their location, beech trees can be found mixed with other deciduous species, in majority downy oak (*Quercus pubescens* Willd., *Quercus petraea* (Matt.) Liebl., Fagaceae), maples (*Acer opalus* Mill., *A. campestre* L., *A. monspessulanum* L., Sapindaceae) and wild cherry-tree (*Prunus avium* L.). Holly (*Ilex aquifolium* L., Aquifoliaceae) can be found throughout the reservation area, and holm oak (*Quercus ilex* L.) is also present. Between 600 and 1000 m, under beech forests, the soils are classified as an association of slightly podzolic acidic brown soils and ochreous brown soils (Favrot *et al.* 1969, Servat & Servant 1972), with some heterogeneity at small spatial scales (Marty 1981).

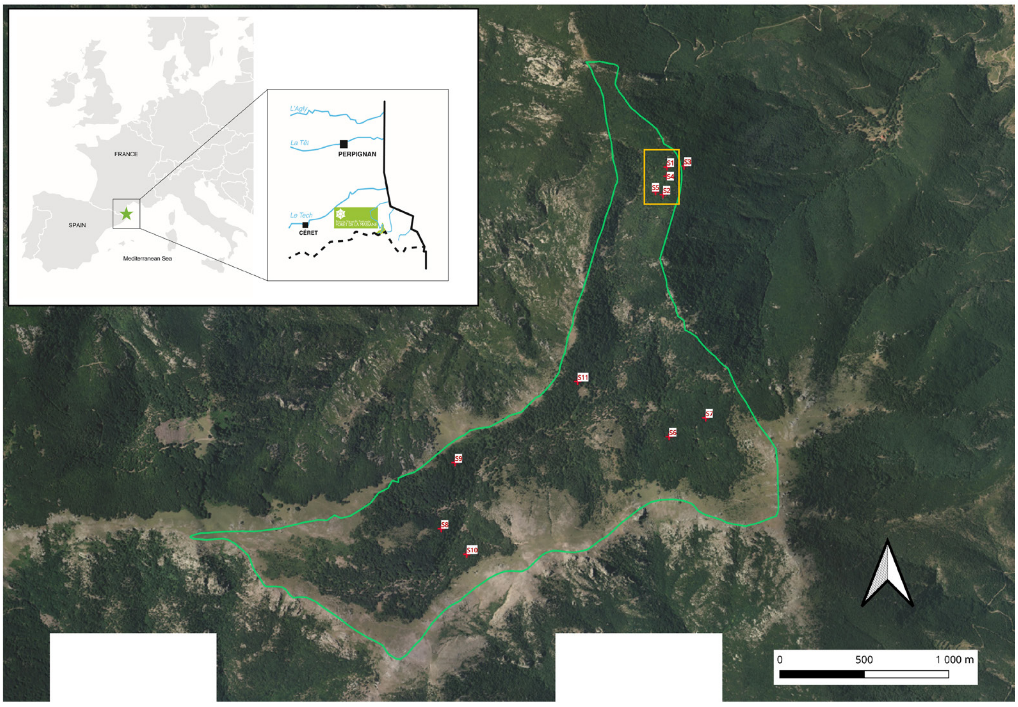

Fig. 1. Situation of the Massane Forest National Nature Reserve (green line) and location of the eleven sampling sites (S1 – S11). The sampling points situated in the historical core reservation zone are positioned within the yellow frame. Map base: BD ORTHO® 5 M © IGN – 2018. Open License V 2.0. FRNC 2023 authorization for public service missions / RNNM.

Sampling sites

Sampling sites were chosen to represent different types of forest stands and facies. Eleven stations (S1-S11) along the Massane Forest National Nature Reserve were selected for soil sampling (Fig. 1). The sampling sites represented mature beech stands (S1, S3, S6-8, S10), populations of beech and oak trees (S2, S4, S5), and mixed forest stands situated within predominantly deciduous oak forests (S9, S11) across a 220 m altitudinal gradient (Table I). Stations S1, S2, S4, and S5 were located within the essential reservation area. S3 was situated only a few meters from this area, allowing for possible cow grazing and walkers to pass through. Mature beech stands included hall-forest stands (Pott 2018, Voloscuk *et al.* 2013) and stands characterized by the presence of very large trees (Larrieu & Gonin 2008, Vandekerkhove *et al.* 2018) represented in our sampling.

Soil sampling

Soil samples were collected in October 2022. The year 2022 was characterized by a rainfall deficit (mean annual rainfall of 693.7 mm) and temperatures exceeding normal values (mean annual temperature of 14.9°C). The pH was measured across the sampling sites and ranged from 5.3 to 4.7 with a median value of 5.2 ± 0.2. Overall soil variables (median values ± sd) indicated the major presence of sandy fractions (coarse sands: 374 ± 73 g/kg, fine sands 192 ± 44 g/kg). The proportion of fine silts (149 ± 18 g/kg) and clay (146 ± 14 g/kg) was equivalent, and the minor fraction was composed of coarse silts (117 ± 14 g/kg). Organic matter represented 111 ± 21 g/kg. Three replicates of mineral soil were collected from each sampling site, positioned at the corners of an equilateral triangle, with sides measuring 1 m. Soil samples were collected using an inox shovel from the first 10 cm of soil depth after removing humus and litter forming the organic layer (if present) to target the A horizon. Similar topsoil sampling has been to study soil chemical composition and microbial communities (Mennicken *et al.* 2020, Quan *et al.* 2022, Tedersoo *et al.* 2016). The shovel was cleaned with absolute ethanol before field sampling and used to sample a false soil core in a radius of 1 m from the sampling points between each sampling site to remove any soil and debris left from the previous point, as described by (Mennicken *et al.* 2020). Each replicate was isolated in 2 oz glass jars (Wheaton, Millville, NJ, USA) calcinated before field sampling to prevent any organic contamination, and kept at -80°C when returning in the laboratory until further processing. Field sampling is illustrated in Fig. 2.

Sampling site	GPS coordinates	Orientation	Altitude (m)	Slope (°)	Stand type*	Observations**
S1	42°29.5680N, 3°1.9300E	W	680	20	B	Mature beech stand "Hall-forest" type
S2	42°29.4740N, 3°1.9270E	W	680	20	B/O	Beech stand of lower height; Occasional presence of oaks
S3	42°29.5450'N, 3°2.0010'E	W	690	20	B	Mature beech stand "Hall-forest" type Noticeable presence of litter
S4	42°29.5340'N, 3°1.9460'E	W	680	20	B/O	Mature beech stand; Occasional presence of oaks
S5	42°29.4840'N, 3°1.9000'E	W	660	20	B/O	Beech stand of lower height; Occasional presence of oaks; Presence of a herbaceous layer and low shrubs
S6	42°28.6990'N, 3°1.9240'E	N	790	25	B	Mature beech stand "Hall-forest" type
S7	42°28.7420'N, 3°2.1050'E	NW	820	30	B	Mature beech stand Presence of very large standing beech trees
S8	42°28.4330'N, 3°0.9970'E	SW	880	30	B	Mature beech stand Predominance of very large standing beech trees (DBH up to 180 cm)
S9	42°28.6140'N, 3°1.02701'E	E	880	35	M	Mixed forest stand Presence of very large maple trees
S10	42°28.3210'N, 3°1.0770'E	W	870	25	B	Mature beech stand Predominance of very large standing beech trees
S11	42°28.8740'N, 3°1.5580'E	E	810	45	M	Mixed forest stand Presence of very large maple trees

* B: beech, O: oak, M: mixed forest stands

** Very large trees: DHB (diameter at breast height) > 70 cm (220 cm of circumference), "hall-forest": uniform forest stand dominated by old individuals of maximum height, and characterized by a closed canopy and the lack of an understory

Table I.- Characteristics of the sampling sites

Fig. 2.- Illustration of the sampling protocol: topsoil collection using an inox shovel and glass jars (left), position of the three replicates.

Soil processing and extraction

Soil processing and sample preparation for metabolomic analysis were conducted based on previously published protocols, with some modifications (Duan *et al.* 2022, Pétriacq *et al.* 2017, Withers *et al.* 2020). All frozen soil samples underwent overnight lyophilization using a freeze dryer (Beta 2-8 LD Plus Freeze Dryer, Martin Christ Gefriertrocknungsanlagen GmbH, Osterode am Harz, Germany). Subsequently, the samples were homogenized by sieving through a 0.5 mm sieve to ensure the removal of any discernible plant components and pebbles. For each sample, approximately 1 g of soil was accurately weighted (with an accuracy of 0.1 mg), placed in Pyrex borosilicate glass round bottom 16×125 culture tubes with screw cap and PTFE lined rubber disc (DWK Life Sciences, Stoke-on-Trent, UK), and covered with the corresponding volume of methanol: isopropanol: water (3:3:2 v/v/v) mixture to achieve a concentration of 0.5 g/ml of soil sample in the solvent. The solution was vortexed for 5 s and placed in an ultrasound bath (Elmasonic S30H, Elma Schmidbauer GmbH, Singen, Germany) at 37 kHz for 20 min to improve the recovery of metabolites. All tubes were rigorously sealed, tilted at 20° to the horizontal, and shaken at 110 rpm for 24 h with an InforsHT Orbitron shaker (Infors AG, Bottmingen, Switzerland), with care taken to prevent the solvent from reaching the tube cap, as described in (Rodrigues *et al.* 2021). The extracts were then centrifuged at 500 G for 10 min (GenevacTM HT4X, Fischer Scientific, Illkirch, France) to pelletize the sample, and the supernatant was transferred directly to a clean vial for UPLC-HRMS/MS analysis.

UHPLC-HRMS/MS analysis

Liquid chromatography – high resolution mass spectrometry analyses were conducted as described in Stien *et al.* (2019) with an Ultimate 3000™ UHPLC system (Thermo Fisher Scientific, Waltham, Ma, USA) coupled to an Orbitrap MS/MS FT Q-Exactive focus mass spectrometer. Analyses of extracts (5 µL injected) were performed in electrospray positive ionization mode (ESI+) in the 133.4 – 2000 Da range in centroid mode. The parameters were as follows: spray voltage: 3 kV, sheath flow rate: 75, aux gas pressure: 20, capillary temperature: 350 °C, heater temperature: 430 °C. The analysis was conducted in FullMS data dependent MS^2 mode (Discovery mode). Resolution was set to 70,000 in FullMS mode, the AGC (automatic gain control) target was set to 3×10^6, and the lock mass option was set for an ion at *m/z* 144.98215, corresponding to $Cu(CH^3CN)^{2+}$ for internal calibration. In dd-MS^2, resolution was 17,500, AGC target was set to $1{\times}10^5$, isolation window was 0.4 Da, and normalized collision energy was stepped to 15, 30 and 45 %, with 6 s dynamic exclusion. The UHPLC column was a Phenomenex Luna Omega Polar C18 1.6 µm, 150×2.1 mm. The column temperature was set to 42 °C, and the flow rate was 0.5 $mL.min^{-1}$. The solvent system was a mixture of water (A) with increasing proportions of acetonitrile (B), with both solvents modified with 0.1 % formic acid. The gradient was as follows: 2 % B 3 min before injection, then from 1 to 15 min, a shark fin gradient increase of B up to 100 % (curve 2), followed by 100 % B for 5 min. Profiles were viewed using FreeStyle® 1.5 software (Thermo Fisher Scientific).

MS/MS molecular networking

Molecular networks consist in the representation of complex molecular data, with ions being presented as nodes that are interconnected according to their structural similarities based on tandem mass spectra. It thus allows the mapping of the chemical diversity observed in untargeted metabolomic analyses, enabling the recognition of patterns and assisting in the structural elucidation of compounds through the annotation of the chemical space (Aron *et al.* 2020, Nothias *et al.* 2020). We used MZmine2 v2.51 to process the UHPLC-MS/MS data obtained from the soil extracts analysis to obtain a feature detection and ion alignment table (Katajamaa *et al.* 2006, Pluskal *et al.* 2010). MZmine2 data were then processed using the Feature-Based Molecular Networking (FBMN) workflow in the GNPS (Global Natural Products Social Molecular Network, https://gnps.ucsd.edu) platform (Wang *et al.* 2016). FBMN is a computational method that bridges mass spectrometry data processing tools for LC-MS/MS and molecular networking (MN) analysis of GNPS (Nothias *et al.* 2020). The FBMN workflow includes a High-Throughput dereplication tool, comprehensive MS/MS libraries, and find analogues of known compounds in the library. This platform compares the MS/MS spectra of unknown metabolites from samples with a library of MS/MS spectra generated from structurally characterized metabolites. The precursor ion mass tolerance was set at 0.01 Da and the MS^2 fragment ion tolerance was set at 0.01 Da. The comparison is based upon the similarity cosine scoring of the MS/MS spectra. The minimum cosine for linking two parent ions was set as 0.7, minimum 8 matched fragment ions and maximum 300 connected component size. The MS^2 spectra in the network were searched against the "GNPS spectra library". All matches between network and library spectra were required to have a score above 0.7 and at least 6 matched peaks. Upon generating the MN, GNPS automatically annotated the compounds present in its databases. Molecular network (MN) images were generated using Cytoscape (https://cytoscape.org/), an open-source MN visualization software (Otasek *et al.* 2019, Shannon *et al.* 2003). For the FBMN analysis, three groups and four subgroups were defined, as presented in Table II. Group 1 included all mature beech stands, the subgroup depending on their location and slope (violet subgroup: in or near the historical core reservation area with low slope, yellow subgroup: other mature beech stands with stronger slope). Group 2 included beech/oak stands and formed two subgroups (red and blue). The blue subgroup, which included only sampling site S5, was isolated because of the strong presence of an understory (herbaceous layer and small shrubs) at this location. Group 3 (green) comprised mixed forest stands. The relative peak area of different parent ions in each group was used to create pie charts in which each portion represents the same node (each node is a cluster of MS^2 spectra that may come from different isomeric protonated molecular ions).

Group	1 - Mature beech						2 - Beech & oak			3 - Mixed	
Subgroup	Violet		Yellow				Red		Blue	Green	
Sampling site	S1	S3	S6	S7	S8	S10	S2	S4	S5	S9	S11

Table II.- Groups and subgroups used for the FBMN molecular network analysis

Quantification of forest soil chemodiversity

For this assessment, features were considered as chemical species and submitted to ecological models for the quantification of their diversity (Andermann *et al.* 2022, Whittaker 1960). The α-diversity was evaluated through species richness and the Shannon index, and complemented by the calculation of the Piélou index. The species richness (S) represents the total number of species presented in each subgroup, without taking into account the relative abundance of each species. The Shannon index (H) considers both species richness and relative abundance. The higher the H index, the greater the diversity. Piélou's evenness index (J) was used to complement these data (Bahnmann *et al.* 2018, Gosselin 2006). A J value of 0 corresponds to the dominance of one of the species, and 1 to the equidistribution of the different species among the communities. Jaccard similarity coefficient was used to assess the β-diversity. This index is calculated between two communities (*i.e.*, two subgroups) and count the proportion of chemical species they share, relying on the presence/absence of the features without taking into account their abundance. The lower the index value, the less similar the specific composition of the communities, the greater the β-diversity is considered to be. Calculation of the biodiversity indices was performed using the *vegan* package (Oksanen *et al.* 2024) in R software version 4.3.2 (https: //www.R-project.org). In this package, the index calculated is a dissimilarity index. Jaccard similarity coefficient is therefore complementary to this dissimilarity index and was calculated as: similarity = 1-dissimilarity. Complementary NMDS graphical representation and associated descriptive and multivariate analyses were performed in R version 4.0.3 (R Development Core Team, 2020) using packages *ggplot2* and *vegan*. For the analyses of the chemical communities, the function *rankindex* was used to rank the performance of different dissimilarity indices. In our case, Bray-Curtis distance was the most relevant dissimilarity index. Effect of soil subgroup on the structure of chemical communities (Hellinger-transformed relative abundances) was tested using permutational multivariate analysis of variance based on Bray-Curtis distance matrix (PERMANOVA: *adonis* function with 999 permutations). The assumption of multivariate homogeneity of variances was checked and validated ($F_{4,28} = 0.88$, $P = 0.48$) following Anderson's PERMDISP2 procedure (*betadisper* function). Pairwise multilevel comparison (*pairwise.adonis* function) was used as posthoc grouping for the PERMANOVA based on Bonferroni's adjusted p-values (Supplementary Materials, Table S1). Nonmetric multidimensional scaling (NMDS) (*metaMDS* function) was used to ordinate samples and species scores as a graphical display of Bray-Curtis dissimilarity distances between groups of samples.

Spectra annotation

For metabolite annotation, two complementary workflows were used. The first approach is automatic, and took into account the annotations proposed by the GNPS Dereplicator tool, the result of which is displayed directly on the molecular networks. Dereplicator is an algorithm for annotating natural products in databases. This tool is based on the comparison of experimental mass spectra with theoretical spectra generated from in silico fragmentation rules, in order to identify fragments common to known metabolites (Allard *et al.* 2016, Mohimani *et al.* 2017).

In addition, we used CANOPUS as a tool for predicting compound classes directly from MS/MS data. CANOPUS runs as a webservice (Djoumbou Feunang *et al.* 2016, Dührkop *et al.* 2021,Kim *et al.* 2021) and is integrated in SIRIUS version 4.4 (Lehrstuhl Bioinformatik, Jena) (Dührkop *et al.* 2019). The objective was to gain general information about the chemical landscape of the forest soil, with a specific interest in the features that could be considered as biomarkers for specific groups or subgroups. These features were characterized by nodes that were predominantly associated with a single or a majority color, thereby underscoring the distinctive compounds related to the type of forest stands. Thus, this analysis concentrated on the ions both present within the principal MNs and related to these specific networks, deliberately excluding orphan ions (226 features) and those found in very small networks (comprising two or three features), unless they were distinctly linked to a particular group or subgroup. The complete dataset used for the construction of the molecular networks with Cytoscape is provided as Supplementary Materials (Table S2).

RESULTS

Quantitative assessment of forest soil chemodiversity

The analysis of the metabolomic profiles of the soil extracts using UHPLC-HRMS/MS and the construction of the molecular networks led to the obtention of 737 features. The range of parent masses per charge (*m/z*) detected, all features combined, extended from 145.1012 to 1803.7458. The chemical diversity for each landscape type, corresponding to the subgroups defined in Table II, was assessed using ecological diversity indices, here applied to the obtained features. These features were thus considered as chemical species among the chemical communities characterizing the subgroups. The evaluation of the α-diversity, corresponding to the intra-subgroup chemodiversity, highlighted similar levels of chemical species richness for each subgroup, with equivalent numbers of chemical species (mean value 719 ± 14, coefficient of variation 0.02), highly diverse chemo-ecosystems (H > 5), and a relatively even distribution of chemical species among the subgroups (J ~ 1 for each subgroup). Results are presented in Table III.

Group / Stand		1 - Mature beech		2 - Beech & oak		3 - Mixed
Subgroup		Violet	Yellow	Red	Blue	Green
	Species richness (S)	726	732	725	697	714
α-diversity	**Shannon index (H)**	5.45	5.35	5.46	5.27	5.38
	Péliou index (J)	0.828	0.811	0.829	0.804	0.819

Table III.- Evaluation of the intra-subgroup chemodiversity

The β-diversity, *i.e.*, the inter-subgroup chemodiversity, was evaluated using the Jaccard similarity coefficient. The distance matrix obtained for the studied subgroups is represented in Table IV. The highest value was of 0.986, calculated between the yellow and violet subgroups both corresponding to mature beech stands. This indicated the highest similarity, and thus the lowest β-diversity in terms of features, among all subgroups. The highest β-diversity, indicated by the lowest index value, was of 0.936 and was calculated between the blue and the green subgroups, corresponding to a mixed beech/oak stand with significant understory and mixed forest stands, respectively. The median value was 0.968. These results indicated an overall similarity between the subgroups in terms of presence/absence of the features, consistent with the high species richness calculated above.

Group / Stand	1 - Mature beech		2 - Beech & oak		3 - Mixed
Subgroup	Violet	Yellow	Red	Blue	Green
Violet	1				
Yellow	0.986	1			
Red	0.977	0.98	1		
Blue	0.947	0.947	0.953	1	
Green	0.975	0.97	0.965	0.936	1

Table IV.- Evaluation of the inter-subgroups chemodiversity (Jaccard similarity coefficient)

The structure of the chemical community was significantly affected by soil subgroups (PERMANOVA, $F_{4,28} = 8.05$, $R^2 = 0.53$, $P < 0.001$). Pairwise multi-level comparisons were all significant, except for the discrimination of the blue subgroup (beech/oak stand with understory), for which a low number of replicates lead to non-significant p-adjusted contrasts with red, violet and green subgroups (Table S2). NMDS display (Fig. 3) was robust (stress-value of 0.1) and consistent with Table IV, highlighting a greater dissimilarity of blue, red and green groups, while yellow and violet groups (soils in mature beech forest stands) superimpose slightly more, suggesting they may share more similar chemical features than with other soils.

Qualitative exploration of forest soil chemical landscapes

The evaluation of the chemical landscape associated to the different subgroups was performed using molecular networks (MNs). The obtained results are represented in Fig. 4. The overall annotation results for compound classes are presented in Table V.

Out of the 737 features identified, 679 were found across all sampling locations, thereby constituting the core metabolome of our experimental framework. GNPS proposed automatic annotations for some of the molecular networks. The MN1 subnetwork exhibited common features that were detected across all subgroups in varying amounts. GNPS automatic annotations proposed linoleic acid and derivatives such as conjugated linoleic acid, 9(10)-EpOME (9,10-cis epoxide of linoleic acid), alongside with other fatty acid (FA) derivatives: mono glycerides (monolinolein, monoolein, mononervonin, monoelaidin, monopalmitolein), FA amides (13-docosenamide, 9-octadecenamide), and a FA alcohol (2,4-dihydroxyheptadecylacetate). Consequently, the MN1 area of the molecular network could be related to fatty acids and fatty acids derivatives. Two annotations, both corresponding to galactosylceramides GalCer(d18:2/16:1), were proposed for the subnetwork MN2, corresponding to sphingolipids (hexosylceramides). The CANOPUS tool was employed to enhance these annotations for MN^2, corroborating the GNPS proposal for 10 of the 12 ubiquitous features, along with the addition of two long-chain ceramides.

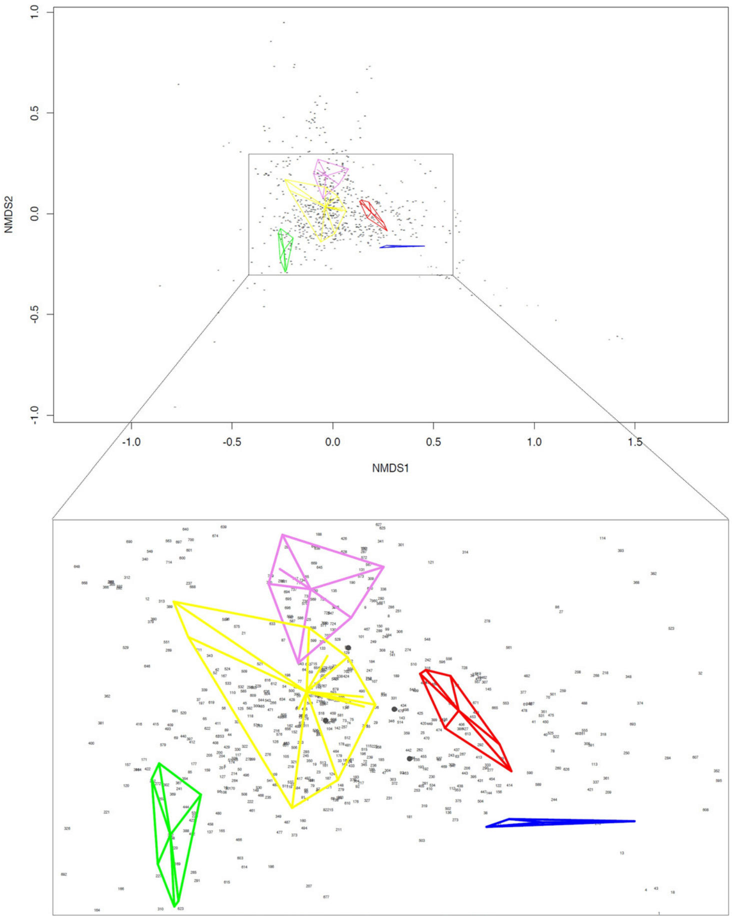

Fig. 3.- Chemical community structure: non-metric multidimensional scaling (NMDS) of chemical (features) communities for each subgroup. Violet subgroup: mature beech stands within the historical core reservation area and surroundings, yellow subgroup: other mature beech stands, red subgroup: beech/oak stands with low to no understory, blue subgroup: beech/oak stands with dense understory, green subgroup: mixed forest stands. Upper section: full NMDS with representation of the enlarged area; lower section: zoomed-in view. Coloured spider webs link sample scores to soil subgroups centroids. Numbers (from 1 to 737, as indicated in Supplementary Materials Table S2) represent the position of chemical species.

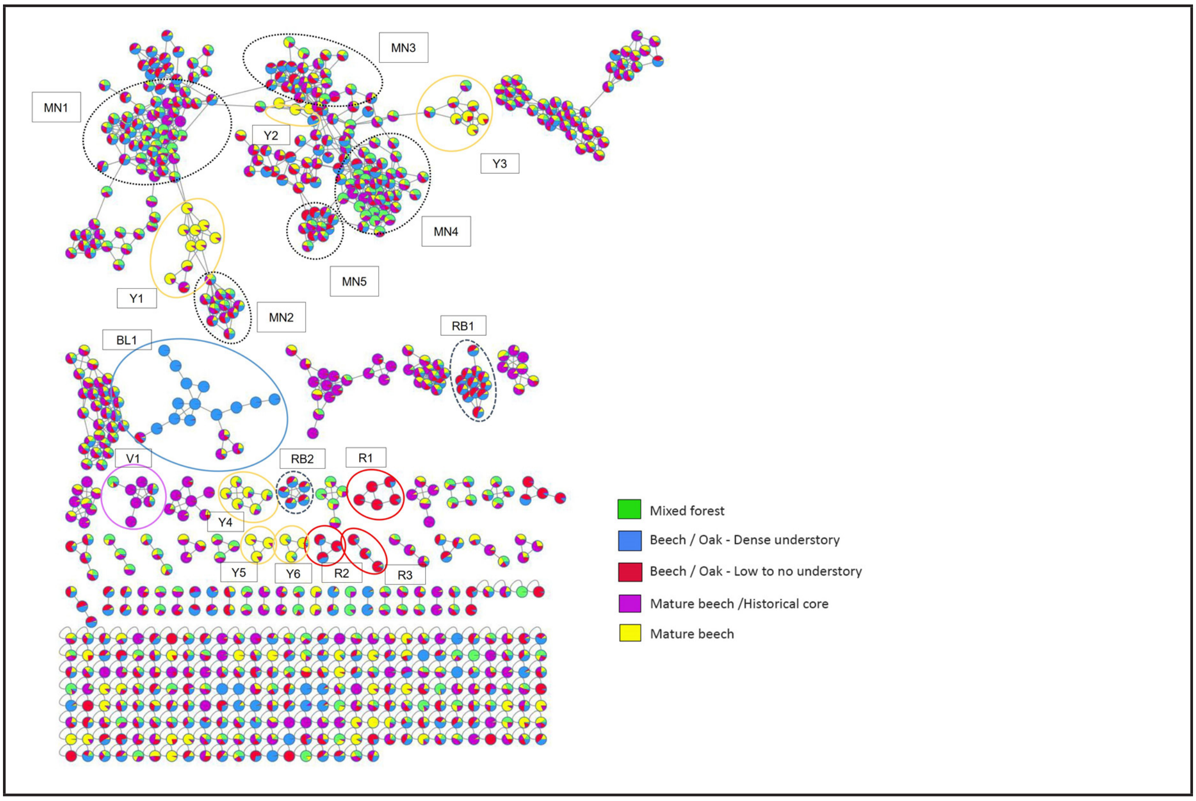

Fig. 4. Molecular networks (MNs) generated with the GNPS Molecular Networking FBMN tool. The nodes color chart represents the proportion of each group for the considered ion, based on peaks area (Group 1: mature beech stands, with violet subgroup: historical core reservation area and surroundings and yellow subgroup: other mature beech stands, Group 2: beech/oak stands, with red subgroup: low to no understory and blue subgroup: dense understory), Group 3 (green nodes): mixed forest stands. Black dotted lines indicate molecular networks including ubiquitous features (present in all groups). Full lines indicate molecular networks associated with a single subgroup (noted in capital letter as the MN reference, VT: violet, Y: yellow, R: red, BL: blue), the color of the line corresponding to the color of the group/subgroup. Grey dashed lines indicate molecular networks related to Group 2 (RB for red/blue).

The molecular subnetwork Y1 was situated between MN1 and MN2, revealing structural closeness. This network comprised nine features predominantly associated with Group 1 (mature beech stands), primarily linked to the yellow subgroup (stands with a strong slope), while also exhibiting some association with the violet subgroup (stands with a low slope). The tenth feature within this network could be related to both Groups 1 and 2 (mixed beech/oak stands). Given that no annotations were provided by GNPS for this network, the spectral data were submitted to SIRIUS for analysis. The examination of the MS^2 data related to Y1 MN through the CANOPUS tool allowed for the annotation of long-chain ceramides (including Cer(14:0/16:1), Cer(14:0/16:0) and Cer(15:0/15:0) as putative annotations), thereby establishing a structural connection between the annotations of MN1 (fatty acids) and MN2 (hexosylceramides and long-chain ceramides).

Group	Subgroup	Molecular network	Compound class
-	-	MN1	Fatty acids and fatty acids derivatives
		MN2	Sphingolipids (hexosylceramides and long-chain ceramides)
		MN3	Triterpenoids (pentacyclic triterpenoids)
		MN4	Triterpenoids (pentacyclic triterpenoids and other triterpenoids)
		MN5	Triterpenoids (pentacyclic triterpenoids)
1	Yellow	Y1	Sphingolipids (long-chain ceramides)
		Y2	Prenol lipids
		Y3	Terpenoids
		Y4	Coumarin derivatives (praeruptorin)
		Y5	Steroids derivatives
		Y6	Coumarin derivatives (pteryxin)
	Violet	V1	Triterpenoids (pentacyclic triterpenoids)
2	Red	R1	Steroids and steroids derivatives
		R2	Triterpenoids (pentacyclic triterpenoids)
		R3	Lipopeptides (halovirs derivatives)
	Blue	BL1	Sesquiterpenes and sesquiterpenes derivatives
	Red + Blue	RB1	Oligopeptides and amino acid derivatives
		RB2	Triterpenoids

Table V.- Automatic (GNPS) and semi-automatic (SIRIUS) annotations

Limited automatic annotations were available for the ubiquitous features of MN3, all of which encompassed pentacyclic triterpenoid compounds, specifically betulin, betulinic acid, 3α-lu-20(29)-en-3-ol and glochidone, an oxo-lupa-1,20(29)-diene derivative. This class of compounds also constituted the majority of the GNPS annotations for MN4, which included oleanolic acid, ursolic acid, asiatic acid, sumaresinolic acid and betulonic acid. Additionally, two other triterpenoids were also automatically annotated in MN4: masticadienoic acid and glycyrrhizic acid, the latter being a triterpene glycoside. Sumaresinolic acid was the sole annotation proposed for several features included in MN5. Complementarily, three features, categorized within the Y2 subnetwork, exhibited structural relationships to both to the lipids network (MN1) and triterpenoids network (MN3), and were consistently annotated by the CANOPUS tool as prenol lipids, which are lipids derived from the condensation of isoprene subunits according to the LIPID MAPS classification (Fahy *et al.* 2011). Eventually, the focus was placed on the Y3 subnetwork, which is composed of 8 features. Six of these features were predominantly attributed to the yellow subgroup, while the remaining two were mostly found across all subgroups. The annotations provided by SIRIUS enabled the classification of these features into the terpenoid class, including ursonic acid.

The analysis of the features specifically or mainly related to the yellow subgroup (mature beech stands with strong slope) was enhanced by the examination of smaller isolated MNs. The GNPS annotations for Y4 MN related these features to coumarin derivatives, likely praeruptorins or analogs. Additionally, GNPS suggested other coumarin derivatives associated with pteryxin as automatic annotations for the three features identified as Y6 MN. The molecular network assigned as Y5, for its part, gathered steroid derivatives.

Regarding the features specifically associated with the violet subgroup (mature beech stands with low slope) in their majority, only the V1 network could be annotated with reliable outcomes using SIRIUS. This analysis allowed to attribute the 7 features to the pentacyclic triterpenoids class, probably with a lupane-type skeleton, with four features being exclusive to the violet subgroup. The remaining violet MNs could not be clearly annotated using either GNPS or SIRIUS for structural proposals.

Only three MNs predominantly associated with the red subgroup of Group 2 (features mostly found in the mixed beech/oak stands devoid of understory, with some additional presence in the blue subgroup, *i.e.*, mixed beech/oak stand with significant understory) could be successfully annotated. The features of R1, R2 and R3 MNs were annotated using SIRIUS as steroids and steroid derivatives, pentacyclic triterpenoids, and lipopeptides (halovirs derivatives), respectively. The remaining red MNs did not yield any concluding result. Furthermore, a single MN was obtained that contained 13 features specifically associated with the blue subgroup, along with four ubiquitous compounds. The GNPS tool provided two automatic annotations: costunolide, a sesquiterpene lactone, and lychnopholic acid, a trioxygenated caryophyllene derivative. Analyzing the MS^2 data using SIRIUS suggested that sesquiterpenes and their derivatives represent the predominant class of compounds within the BL1 network, aligning with the findings from GNPS, and with xylaric acid, viscic acid and eudesmane derivatives as putative annotations. Eventually, two mixed red/blue networks, thus characterizing Group 2 general chemical diversity, were investigated using the CANOPUS tool, to reveal the presence of amino acid related compounds (RB1, oligopeptides and amino acid derivatives) and triterpenoids (RB2), respectively.

No ions were detected only in the samples originating from the mixed forest stands (green subgroup), and thus specifically related to this type of forest facies. All features detected in these samples were also detected elsewhere.

DISCUSSION

The examination of spatial patterns within a given ecosystem is essential for advancing our understanding of its functioning and revealing the interactions and processes that contribute to its structure (Truchy *et al.* 2019, Whittaker *et al.* 2001). This methodology, when applied to the chemical communities formed by the molecular species present in each forest type of our sampling, demonstrated high chemical richness and unexpected relative chemical homogeneity among the different types of forest stands. These results can be interestingly compared to those from early research in the field of ecological microbiology, linking environmental heterogeneity and fungal diversity in topsoils (Bahram *et al.* 2015). A recent investigation regarding biodiversity and ecosystem functioning (BEF) has also underscored a positive effect of tree diversity and a contribution of species heterogeneity on aboveground biomass, thereby emphasizing the significance of forest type on BEF, especially at small scales (Yao *et al.* 2023). In this perspective, our results (high chemical richness in each subgroup and a well-represented core metabolome across all sites) could also suggest the presence of a “mature” chemodiversity with regard to the maturity of the Massane forest, with an overall climacic chemical landscape corresponding to this undisturbed forest ecosystem. Furthermore, the assessment of biodiversity and ecosystem multifunctionality (BEMF) showed an indirect effect of forest stand spatial structure, evaluated through canopy height, vertical foliage distribution and DBH distribution, on soil multifunctionality (including carbon, nitrogen and calcium content, pH or enzymatic activity), through soil microbial diversity (Zhou *et al.* 2024). Thus, a deeper characterization of the various sampling sites, notably based on an index of biodiversity potential (Larrieu & Gonin 2008, Zeller *et al.* 2022) could provide valuable information. In our case, it is however important to note that the quantitative assessment of chemical richness in forest soil relied solely on the presence/absence of the features, without considering their chemical nature or structural specificities. This is why molecular networks were useful, allowing for the exploration of both spatial and qualitative structural molecular heterogeneity.

The results given by the molecular networks can be discussed both in terms of the nature of chemical classes and their distribution across the sampling sites. The larger and more diverse compound classes (lipids, terpenoids, oligopeptides and phenylpropanoids) are overall consistent with previously published studies (Brown *et al.* 2024, Song *et al.* 2024). In our case, lipids represented an important part of the molecular species annotated within the networks. Linoleic acid and several related compounds were annotated among the fatty acid group of the MN1 molecular subnetwork. This polyenoic acid has already been shown to be associated with fungal occurrence in soils, for example representing 34 to 88 % of the total FA content of fungal biomass from different soil fungi (ascomycetes, basidiomycetes and mitosporic fungi) from various forest types (Ruess *et al.* 2002). Even if this FA can also be found in plants and animals, it can be assumed that the microbial, and notably fungal origin, is predominant (Ding *et al.* 2020, Ruess & Chamberlain 2010). Moreover, this FA is frequently used as a fungal biomarker, notably for ectomycorrhizal fungi (Högberg 2006, Lucas-Borja *et al.* 2012, Olsson 2006). In terms of ecological functions, the large presence of this essential polyunsaturated FA also suggests a strong potential of the Massane forest soil to harbour a wide diversity of detritivorous or fungivorous invertebrates that will form a complex food web and contribute to the overall forest biodiversity (Digel *et al.* 2014).

Among the compounds automatically annotated in MN1 also stood 9(10)-EpOME, which is derived from the oxidation of linoleic acid, FA amides such as 13-docosenamide, and monoacylglycerols. The oxylipin compound 9(10)-EpOME is a signaling molecule involved in defense mechanisms and is present in various taxa, including plant, fungi, or bacteria (Beccaccioli *et al.* 2022, Lombardi *et al.* 2018, Parks *et al.* 2022). 13-Docosenamide was notably detected in citrus root exudates, with a reduced relative abundance in the case of mycorrhizal fungal inoculation (Cheng *et al.* 2022), and highlighted as a significant compound in the plant-microbial feedback during tobacco cultivation (Shen *et al.* 2020). Additionally, certain monoacylglycerols have been identified as components of root waxes at the plant-rhizosphere interface (Li *et al.* 2007). These examples underscore the importance of soil metabolites, and notably lipids, in facilitating communication between plants and their surrounding environment, particularly with microbial entities (Macabuhay *et al.* 2022).

Some sphingolipids, mainly hexosylceramides, were also annotated as ubiquitous compounds in the different types of forest stands, and categorized within MN2. Hexosylceramides have been sourced from both plant root metabolites and microbial origin. In both instances, they have been demonstrated to play a role in the lipid remodeling response following stress events, specifically in reaction to salinity for root metabolites (Sarabia *et al.* 2020) and drying-rewetting sequences for those of microbial origin (Couvillion *et al.* 2023). Among the sphingolipid class, long-chain ceramides were particularly remarkable in our study, as they were solely identified in the Y1 subnetwork. The annotation of the Y1 features as long-chain ceramides by the CANOPUS tool is consistent with regard to the propagation of the annotations between MN1, MN2 and Y1. Long-chain ceramides were thus strictly associated to mature beech stands, and more specifically those characterized by a strong slope. Such compounds were well represented in the drying-rewetting soil metabolome investigation performed by (Couvillion *et al.* 2023). Some original ceramides annotated in this previously published study and characterized by the 2'-hydroxylation of the FA chain were associated with the genus *Vicinamibacteraceae* and phylum Acidobacteriota, and their elevated level in dry soils inferred to be related to their role in the drought resilience of the microbial taxa that are capable of producing them. The phylum Acidobacteriota, known for its contribution to degradation in forest soils, has been identified as part of the bacterial phyla present in the soil of beech forest stands across multiple studies. It may have been shown to represent a predominant phylum, however, its abundance did not significantly differ when compared to other tree species (Dahl *et al.* 2023, Nacke *et al.* 2016, Staszel-Szlachta *et al.* 2024). A recent metabo-lipidomics investigation of a perennial grass root exudates also highlighted long-chain ceramides as an important class among the annotated compounds (Couvillion *et al.* 2024). Therefore, further investigation should be undertaken, both concerning the structural elucidation of these specific compounds, as well as their biological origin, notably with regard to beech settlements. In particular, the structural relationship between the ubiquitous hexosylceramides and the beech-specific long chain ceramides should be explored through a comprehensive annotation effort.

Prenol lipids and some steroids were also specifically linked to mature beech stand in our analysis, and steroids and related compounds in beech/oak stands. Both groups of compounds were highlighted among the metabolites annotated by (Couvillion *et al.* 2024) in wheatgrass root exudates. It could thus be of significant interest to investigate either the metabolome of beech root exsudates or the metabolites associated with a grassy layer in such forest stands. However, prenol lipids, steroids and derivatives, and notably sterols, can also be of microbial origin (Hoshino & Gaucher 2021, Lindsay *et al.* 2023, van Tilburg *et al.* 2022). Therefore, the structure of these lipidic compounds should be explored, to elucidate the chemical discrepancy between the metabolites specifically found in mature beech stands and mixed oak/beech stands, respectively, in relation to their biological origin.

Terpenoids constituted the subnetworks MN3 to MN5, and have already been highlighted in several soil studies as compounds from vegetal origin. Notably, pentacyclic triterpenoids including compounds of the oleanane, ursane and lupane groups have been annotated in various surface soils from the Tibetan plateau and shown to be related with the surrounding vegetation (Bai *et al.* 2020). Moreover, betulinic acid, oleanolic acid, and ursolic acid were identified as allelopathic compounds related to the tropical tree *Alstonia scholaris*

(L.) R.Br. (Apocynaceae), and having an influence on the growth of neighboring plants (Wang *et al.* 2014). Eventually, terpenoids were among the main chemical classes identified in bulk and rhizospheric soil compartments in an investigation of the *Eucalyptus grandis – Pisolithus albus* (plant host -fungus) interaction (Wong-Bajracharya *et al.* 2020). Thus, and even if some terpenoid structures of microbial origin can also be found (Avalos *et al.* 2022, Cvejic *et al.* 2000), MN3-MN5 subnetworks can be related to compounds of plant origin, possibly with allelochemical effect, according to the annotations proposed by GNPS and SIRIUS tools.

Interestingly, other ursonic acid derivatives (Y3) and lupane-type pentacyclic triterpenoids (V1) were uniquely linked to the soil chemodiversity of mature beech stands. Additionally, some triterpenoids were only found in the mixed beech/oak stands (R2, RB2), while sesquiterpene derivatives were specifically associated with mixed beech/oak stands with significant understory (BL1). This indicates the existence of unique structural compounds characteristic of these specific forest settlements and underscores the need for further exploration of the terpenoid chemical landscape within the forest soil (Hosseini & Pereira 2023, Zeng *et al.* 2019).

The last networks specifically related to a particular forest stand comprised oligopeptides (R3, RB1) and phenylpropanoids, particularly coumarin derivatives (Y4, Y6). Peptides were notably detected in rainforest soil as markers of drought impact, with a lower presence during drought experiments (Hildebrand *et al.* 2023). Oligopeptides, in particular, are known to be related to microbial communities (Brown *et al.* 2024). More specifically, halovirs, which belong to the lipopeptaibol compounds, were shown to be produced by microorganisms, including soil fungi, and displayed antimicrobial activities (Liu *et al.* 2020, Rogozhin *et al.* 2018). Coumarins, on the other hand, are produced by plants and have been identified as components of root exudates, playing a role both in plant iron intake and as semiochemicals, shaping root microbiome in the context of plant-soil feedback (Couvillion *et al.* 2024, Harbort *et al.* 2020, Stringlis *et al.* 2019).

This study aligns with recent advancements in the field of metabolomics, which examine chemodiversity on a landscape-scale in relation to phylogeny, species distribution or plant environment (Defossez *et al.* 2021, Dussarrat *et al.* 2022). Chomel *et al.* (2016) also proposed the development of "ecometabolomics" as a means to apply metabolomics to ecology and advance our knowledge in this field. The metabolites could therefore be envisioned in terms of chemical communities and, reciprocally, be subjected to community ecology concepts and methodologies such as proposed by (Danczak *et al.* 2020) through the "meta-metabolome ecology". As well, taking into account the biochemical and structural properties of the metabolites is fundamental to gain insight into the importance of chemodiversity along with quantitative approaches (Petrén *et al.* 2023). Thus, metabolomics can enable the exploration of a wide range of metabolites for soil chemical characterization, expanding the knowledge of the chemical language that underlies plant-microbe-soil interactions and complementing studies of soil microbiome diversity (Buyer *et al.* 2019, Willers *et al.* 2016). There is also an increasing focus on the response of forest ecosystems to global change, notably amplifying drought events (Peñuelas *et al.* 2017). The influence of stand composition on forest resilience is in particular taken into account (Jourdan *et al.* 2020). In this context, old-growth forests, especially those in the Mediterranean area, are thus gaining attention due to their role in the mitigating of this phenomenon, and serving as refuge areas for biodiversity (Colangelo *et al.* 2021). Therefore, using metabolomics to explore the structure and functions of the chemical landscape of old-growth forests, through a transdisciplinary approach that integrates chemistry, forest science, microbiology and ecology in a holistic perspective, will enhance our understanding of the "wholeness, connectedness and ordered complexity" (Naveh 2000) inherent in forest ecosystems. Investigating how the forest landscape mosaic translate into a chemical landscape mosaic could open innovative perspectives and contribute to the development of the new tools called upon to answer questions at the wide scale of dynamic and interacting ecosystems.

Finally, the exploration of the soil chemical landscape within the Massane forest has revealed an elevated richness in chemical species, highly diverse chemo-ecosystems, and linked landscape heterogeneity and chemical diversity. These findings also enhance previous studies that examined the connections between variations in soil microbial metabolic activity, diversity or community structure, and differences in the aboveground plant community. Besides a core metabolome consisting principally of lipids (fatty acid and derivatives and sphingolipids) and pentacyclic terpenoid compounds, our data highlighted the existence of unique chemical structures related to certain types of forest stands. Notably, mature beech stands soil samples exhibited long-chain ceramides, prenol lipids, and coumarins, in addition to specific steroids and terpenoids. Conversely, the mixed beech/oak stands were associated with steroids and terpenoids networks, including sesquiterpenes, and characterized by the presence of oligopeptides in soil samples. Regarding their biological origin, lipids may originate from both microorganisms and plants, with linoleic acid and derivatives being markers of significant fungal presence. Additionally, some annotated compounds could be distinctly attributed to either plant sources (terpenoids, coumarins) or microbial, notably fungal, origin (oligopeptides). Overall, the function of these compounds in stress response, signalling, or more generally plant-microbe interactions, was illustrated. Continuing the annotation effort to unravel the precise structures of these metabolites could thus provide valuable insights into the intricate networks and operational mechanisms of soil. In this regard, metabolomics thus reveals itself as a powerful tool to explore both the nature and functions of soil metabolites, linking the heterogeneous spatial structure of landscapes, metabolites, and microbial communities, in complement with microbiology and metabarcoding approaches. This knowledge would enhance our ability to assess and predict soil functions in the face of global changes, with the definition of "chemical traits" related to landscape structure and dynamics, all within the context of the Massane forest's cultural heritage and ecological legacy.

ACKNOWLEDGEMENTS. The authors thank the Bio2Mar platform (http://bio2mar.obs-banyuls.fr) for providing access to instrumentation. This work benefited from the financial support of the Fédération des Réserves Naturelles Catalanes (FRNC).

REFERENCES

Allard P-M, Péresse T, Bisson J, Gindro K, Marcourt L, Pham VC, Roussi F, Litaudon M, Wolfender JL 2016. Integration of molecular networking and in-silico MS/MS fragmentation for natural products dereplication. *Anal Chem* 88(6): 3317-3323. https://doi.org/10.1021/acs.analchem.5b04804

Andermann T, Antonelli A, Barrett RL, Silvestro D 2022. Estimating alpha, beta, and gamma diversity through deep learning. *Front Plant Sci* 13: 839407. https://doi.org/10.3389/fpls.2022.839407

Aron AT, Gentry EC, McPhail KL, Nothias LF, Nothias-Esposito M, Bouslimani A, Petras D, Gauglitz JM, Sikora N, Vargas F, van der Hooft JJJ, Ernst M, Kang KB, Aceves CM, Caraballo-Rodríguez AM, Koester I, Weldon KC, Bertrand S Roullier C, Sun K, Tehan RM, Boya CA, Christian MH, Gutiérrez M, Ulloa AM, Mora JAT, Mojica-Flores R, Lakey-Beitia J, Vásquez-Chaves V, Zhang Y, Calderón AI, Tayler N, Keyzers RA, Tugizimana F, Ndlovu N, Aksenov AA, Jarmusch AK, Schmid R, Truman AW, Bandeira N, Wang, Dorrestein PC 2020. Reproducible molecular networking of untargeted mass spectrometry data using GNPS. *Nat Protoc* 15(6): 1954-1991. https://doi.org/10.1038/s41596-020-0317-5

Avalos M, Garbeva P, Vader L, Van Wezel GP, Dickschat JS, Ulanova D 2022. Biosynthesis, evolution and ecology of microbial terpenoids. *Nat Prod Rep* 39(2): 249-272. https://doi.org/10.1039/d1np00047k

Bahnmann B, Mašínová T, Halvorsen R, Davey ML, Sedlák P, Tomšovský M, Baldrian P 2018. Effects of oak, beech and spruce on the distribution and community structure of fungi in litter and soils across a temperate forest. *Soil Biol Biochem* 119: 162-173. https://doi.org/10.1016/j.soilbio.2018.01.021

Bahram M, Peay KG, Tedersoo L 2015. Local-scale biogeography and spatiotemporal variability in communities of mycorrhizal fungi. *New Phytol* 205(4): 1454-1463. https://doi.org/10.1111/nph.13206

Bai Y, Chen Q, Zhou Y, Fang X, Liu X 2020. Terpenoids in surface soils from different ecosystems on the Tibetan Plateau. *Org Geochem* 150: 104125. https://doi.org/10.1016/j.orggeochem.2020.104125

Baldrian P 2017. Forest microbiome: Diversity, complexity and dynamics. *FEMS Microbiol Rev* 41(2): 109–130. https://doi.org/10.1093/femsre/fuw040

Beccaccioli M, Pucci N, Salustri M, Scortichini M, Zaccaria M, Momeni B, Loreti S, Reverberi M, Scala V 2022. Fungal and bacterial oxylipins are signals for intra- and inter-cellular communication within plant disease. *Front Plant Sci* 13: 823233. https://doi.org/10.3389/fpls.2022.823233

Bonfante P, Genre A 2015. Arbuscular mycorrhizal dialogues: Do you speak "plantish" or "fungish"? *Trends Plant Sci* 20(3): 150-154. https://doi.org/10.1016/j.tplants.2014.12.002

Brown RW, Reay MK, Centler F, Chadwick DR, Bull ID, McDonald JE, Evershed RP, Jones DL 2024. Soil metabolomics - current challenges and future perspectives. *Soil Biol Biochem* 193: 109382. https://doi.org/10.1016/j.soilbio.2024.109382

Buyer JS, Vinyard B, Maul J, Selmer K, Lupitskyy R, Rice C, Roberts DP 2019. Combined extraction method for metabolomic and PLFA analysis of soil. *Appl Soil Ecol* 135: 129-136. https://doi.org/10.1016/j.apsoil.2018.11.012

Cateau E, Larrieu L, Vallauri D, Savoie JM, Touroult J, Brustel H 2015. Ancienneté et maturité : Deux qualités complémentaires d'un écosystème forestier. *C R Biol* 338(1): 58-73. https://doi.org/10.1016/j.crvi.2014.10.004

Cheng HQ, Giri B, Wu QS, Zou YN, Kuča K 2022. Arbuscular mycorrhizal fungi mitigate drought stress in citrus by modulating root microenvironment. *Arch Agron Soil Sci* 68(9): 1217-1228. https://doi.org/10.1080/03650340.2021.1878497

Chomel M, Guittonny-Larchevêque M, Fernandez C, Gallet C, DesRochers A, Paré D, Jackson BG, Baldy V 2016. Plant secondary metabolites: a key driver of litter decomposition and soil nutrient cycling. *J Ecol* 104(6): 1527-1541. https://doi.org/10.1111/1365-2745.12644

Colangelo M, Camarero JJ, Gazol A, Piovesan G, Borghetti M, Baliva M, Gentilesca T, Rita A, Schettino A, Ripullone F 2021. Mediterranean old-growth forests exhibit resistance to climate warming. *Sci Total Environ* 801: 149684. https://doi.org/10.1016/j.scitotenv.2021.149684

Couvillion S, Danczak R, Naylor D, Smith ML, Stratton KG, Paurus VL, Bloodsworth KJ, Farris Y, Schmidt DJ, Richardson RE, Bramer LM, Fansler SJ, Nakayasu ES, McDermott JE, Metz TO, Lipton MS, Jansson JK, Hofmockel KS 2023. Rapid remodeling of the soil lipidome in response to a drying-rewetting event. *Microbiome* 11(1): 34. https://doi.org/10.1186/s40168-022-01427-4

Couvillion S, Yang I, Hermosillo D, Eder J, Bell S, Hofmockel K 2024. Chemodiversity in root exudates: A comprehensive characterization of the exudate metabo-lipidome in a perennial grass. *BioRxiv* 586263. https://doi.org/10.1101/2024.03.22.586263

Cvejic JH, Putra SR, El-Beltagy A, Hattori R, Hattori T, Rohmer M 2000. Bacterial triterpenoids of the hopane series as biomarkers for the chemotaxonomy of *Burkholderia*, *Pseudomonas* and *Ralstonia* spp. *FEMS Microbiol Lett* 183(2): 295-299. https://doi.org/10.1111/j.1574-6968.2000.tb08974.x

Dahl MB, Kreyling J, Petters S, Wang H, Mortensen MS, Maccario L, Sørensen SJ, Urich T, Weigel R 2023. Warmer winters result in reshaping of the European beech forest soil microbiome (bacteria, archaea and fungi) - With potential implications for ecosystem functioning. *Environ Microbiol* 25(6): 1118-1135. https://doi.org/10.1111/1462-2920.16347

Danczak RE, Chu RK, Fansler SJ, Goldman AE, Graham EB, Tfaily MM, Toyoda J, Stegen JC 2020. Using metacommunity ecology to understand environmental metabolomes. *Nat Commun* 11: 6369. https://doi.org/10.1038/s41467-020-19989-y

Defossez E, Pitteloud C, Descombes P, Glauser G, Allard P, Walker T, Fernandez-Conradi P, Wolfender JL, Pellissier L, Rasmann S 2021. Spatial and evolutionary predictability of phytochemical diversity. *PNAS* 118(3): e2013344118. https://doi.org/10.1073/pnas.2013344118/-/DCSupplemental

Delamare Deboutteville C, Petit G, Travé J 1957. Introduction à l'étude de la Réserve Naturelle de la Massane. *Vie Milieu* vol VIII (3): 221-234

Delcourt HR, Delcourt PA 1988. Quaternary landscape ecology: Relevant scales in space and time. *Landsc Ecol* 2: 23-44. https://doi.org/10.1007/BF00138906

Delory BM, Callaway RM, Semchenko M 2024. A trait-based framework linking the soil metabolome to plant–soil feedbacks. *New Phytol* 241(5): 1910-1921. https://doi.org/10.1111/nph.19490

Digel C, Curtsdotter A, Riede J, Klarner B, Brose U 2014. Unravelling the complex structure of forest soil food webs: Higher omnivory and more trophic levels. *Oikos* 123(10): 1157-1172. https://doi.org/10.1111/oik.00865

Ding S, Lange M, Lipp J, Schwab VF, Chowdhury S, Pollierer MM, Krause K, Li D, Kothe E, Scheu S, Welti R, Hinrichs KU, Gleixner G 2020. Characteristics and origin of intact polar lipids in soil organic matter. *Soil Biol Biochem* 151: 108045. https://doi.org/10.1016/j.soilbio.2020.108045

Djoumbou Feunang Y, Eisner R, Knox C, Chepelev L, Hastings J, Owen G, Fahy E, Steinbeck C, Subramanian S, Bolton E, Greiner R, Wishart DS 2016. ClassyFire: automated chemical classification with a comprehensive, computable taxonomy. *J Cheminform* 8: 61. https://doi.org/10.1186/s13321-016-0174-y

Duan M, Lu M, Lu J, Yang W, Li B, Ma L, Wang L 2022. Soil chemical properties, metabolome, and metabarcoding give the new insights into the soil transforming process of fairy ring fungi *Leucocalocybe mongolica*. *J Fungi* 8(7): 680. https://doi.org/10.3390/jof8070680

Dührkop K, Felix Nothias L, Fleischauer M, Ludwig M, Hoffmann MA, Rousu J, Dorrestein PC, Böcker S 2021. Systematic classification of unknown metabolites using high-resolution fragmentation mass spectra. *Nat Biotechnol* 39: 462-471. https://doi.org/10.1101/2020.04.17.046672

Dührkop K, Fleischauer M, Ludwig M, Aksenov AA, Melnik AV, Meusel M, Dorrestein PC, Rousu J, Böcker S 2019. SIRIUS 4: a rapid tool for turning tandem mass spectra into metabolite structure information. *Nat Methods* 16: 299-302. https://doi.org/10.1038/s41592-019-0344-8

Dussarrat T, Prigent S, Latorre C, Bernillon S, Flandin A, Díaz FP, Cassan C, Van Delft P, Jacob D, Varala K, Joubes J, Gibon Y, Rolin D, Gutiérrez RA, Pétriacq P 2022. Predictive metabolomics of multiple Atacama plant species unveils a core set of generic metabolites for extreme climate resilience. *New Phytol* 234(5): 1614-1628. https://doi.org/10.1111/nph.18095

Fahy E, Cotter D, Sud M, Subramaniam S 2011. Lipid classification, structures and tools. *Biochim Biophys Acta Mol Cell Biol Lipids* 1811(11): 637-647. https://doi.org/10.1016/j.bbalip.2011.06.009

Favrot J-C, Servan J, Servat E 1969. Les sols du massif des Albères (Pyrénées-Orientales). *Rev For Fr* 21: 619-630. https://doi.org/10.4267/2042/20311ï

Fiehn O 2002. Metabolomics - The link between genotypes and phenotypes. *Plant Mol Biol* 48(1-2): 155-171. https://doi.org/10.1023/A:1013713905833

Fierer N 2017. Embracing the unknown: Disentangling the complexities of the soil microbiome. *Nat Rev Microbiol* 15(10): 579-590. https://doi.org/10.1038/nrmicro.2017.87

Forman RTT, Godron M 1986. Landscape Ecology. Wiley, 619 p.

Gillespie LM, Hättenschwiler S, Milcu A, Wambsganss J, Shihan A, Fromin N 2021. Tree species mixing affects soil microbial functioning indirectly via root and litter traits and soil parameters in European forests. *Funct Ecol* 35(10): 2190-2204. https://doi.org/10.1111/1365-2435.13877

Gosselin F 2006. An assessment of the dependence of evenness indices on species richness. *J Theor Biol* 242(3): 591-597. https://doi.org/10.1016/j.jtbi.2006.04.017

Harbort CJ, Hashimoto M, Inoue H, Niu Y, Guan R, Rombolà AD, Kopriva S, Voges MJEEE, Sattely ES, Garrido-Oter R, Schulze-Lefert P 2020. Root-secreted coumarins and the microbiota interact to improve iron nutrition in *Arabidopsis*. *Cell Host Microbe* 28(6): 825-837. https://doi.org/10.1016/j.chom.2020.09.006

Hildebrand GA, Honeker LK, Freire-Zapata V, Ayala-Ortiz C, Rajakaruna S, Fudyma J, Daber LE, Amini Tabrizi R, Chu RL, Toyoda J, Flowers SE, Hoyt DW, Hamdan R, Gil-Loaiza J, Shi L, Dippold MA, Ladd SN, Werner C, Meredith LK, Tfaily MM 2023. Uncovering the dominant role of root metabolism in shaping rhizosphere metabolome under drought in tropical rainforest plants. *Sci Total Environ* 899: 165689. https://doi.org/10.1016/j.scitotenv.2023.165689

Högberg MN 2006. Discrepancies between ergosterol and the phospholipid fatty acid 18:2ω6,9 as biomarkers for fungi in boreal forest soils. *Soil Biol Biochem* 38: 3431-3435. https://doi.org/10.1016/j.soilbio.2006.06.002

Hoshino Y, Gaucher EA 2021. Evolution of bacterial steroid biosynthesis and its impact on eukaryogenesis. *PNAS* 118(25): e2101276118. https://doi.org/10.1073/pnas.2101276118/-/DCSupplemental

Hosseini M, Pereira DM 2023. The chemical space of terpenes: Insights from data science and AI. *Pharmaceuticals* 16(2): 202. https://doi.org/10.3390/ph16020202

Hu L, Robert CAM, Cadot S, Zhang X, Ye M, Li B, Manzo D, Chervet N, Steinger T, Van Der Heijden MGA, Schlaeppi K, Erb M 2018. Root exudate metabolites drive plant-soil feedbacks on growth and defense by shaping the rhizosphere microbiota. *Nat Commun* 9: 2738. https://doi.org/10.1038/s41467-018-05122-7

Jourdan M, Kunstler G, Morin X 2020. How neighbourhood interactions control the temporal stability and resilience to drought of trees in mountain forests. *J Ecol* 108: 666-677. https://doi.org/10.1111/1365-2745.13294

Katajamaa M, Miettinen J, Orešič M 2006. MZmine: Toolbox for processing and visualization of mass spectrometry based molecular profile data. *Bioinformatics* 22(5): 634-636. https://doi.org/10.1093/bioinformatics/btk039

Kim HW, Wang M, Leber CA, Nothias LF, Reher R, Kang KB, Van Der Hooft JJJ, Dorrestein PC, Gerwick WH, Cottrell GW 2021. NPClassifier: A deep neural network-based structural classification tool for natural products. *J Nat Prod* 84(11): 2795-2807

Larrieu L, Gonin P 2008. L'indice de biodiversité potentielle (IBP) : une méthode simple et rapide pour évaluer la biodiversité potentielle des peuplements forestiers. *Rev For Fr* 60(6): 727-748. https://doi.org/10.4267/2042/28373ï

Li Y, Beisson F, Ohlrogge J, Pollard M 2007. Monoacylglycerols are components of root waxes and can be produced in the aerial cuticle by ectopic expression of a suberin-associated acyltransferase. *Plant Physiol* 144(3): 1267-1277. https://doi.org/10.1104/pp.107.099432

Lindsay CA, Kinghorn AD, Rakotondraibe HL 2023. Bioactive and unusual steroids from *Penicillium fungi*. *Phytochem* 209: 113638. https://doi.org/10.1016/j.phytochem.2023.113638

Liu R, Khan RAA, Yue Q, Jiao Y, Yang Y, Li Y, Xie B 2020. Discovery of a new antifungal lipopeptaibol from *Purpureocillium lilacinum* using MALDI-TOF-IMS. *Biochem Biophys Res Commun* 527(3): 689-695. https://doi.org/10.1016/j.bbrc.2020.05.021

Lombardi N, Vitale S, Turr ÀD, Reverberi M, Fanelli C, Vinale F, Marra R, Ruocco M, Pascale A, D'Errico G, Woo SL, Lorito M 2018. Root exudates of stressed plants stimulate and attract trichoderma soil fungi. *MPMI* 31(10): 982-994. https://doi.org/10.1094/MPMI-12-17-0310-R

Lucas-Borja ME, Candel D, Jindo K, Moreno JL, Andrés M, Bastida F 2012. Soil microbial community structure and activity in monospecific and mixed forest stands, under Mediterranean humid conditions. *Plant Soil* 354: 359-370. https://doi.org/10.1007/s11104-011-1072-8

Macabuhay A, Arsova B, Walker R, Johnson A, Watt M, Roessner U 2022. Modulators or facilitators? Roles of lipids in plant root–microbe interactions. *Trends Plant Sci* 27(2): 180-190. https://doi.org/10.1016/j.tplants.2021.08.004

Magri D 2008. Patterns of post-glacial spread and the extent of glacial refugia of European beech (*Fagus sylvatica*). *J Biogeogr* 35(3): 450-463. https://doi.org/10.1111/j.1365-2699.2007.01803.x

Majdi N, Araujo TQ, Bekkouche N, Fontaneto D, Garrigue J, Larrieu L, Kamburska L, Kieneke A, Minowa AK, Laumer C, Sabatino R, Sorel D, Stec D, Traunspurger W 2024. Freshwater and limno-terrestrial meiofauna of the Massane Forest Reserve in the Eastern French Pyrenees. *Biogeographia* 39(1): a032. https://doi.org/10.21426/B639162226

Marty M-C 1981. Réserve Naturelle de la Massane - Travaux 9 - Etude pédologique. Masters' thesis, Université Paul Sabatier

Mennicken S, Kondratow F, Buralli F, Manzi S, Andrieu E, Roy M, Brin A 2020. Effects of past and present-day landscape structure on forest soil microorganisms. *Front Ecol Evol* 8: 118. https://doi.org/10.3389/fevo.2020.00118

Mhlongo MI, Piater LA, Madala NE, Labuschagne N, Dubery IA 2018. The chemistry of plant–microbe interactions in the rhizosphere and the potential for metabolomics to reveal signaling related to defense priming and induced systemic resistance. *Front Plant Sci* 9: 112.

https://doi.org/10.3389/fpls.2018.00112

Mithöfer A, Boland W 2016. Do you speak chemistry? *EMBO Rep* 17:626-629. https://doi.org/10.15252/embr.201642301

Mohimani H, Gurevich A, Mikheenko A, Garg N, Nothias LF, Ninomiya A, Takada K, Dorrestein PC, Pevzner PA 2017. Dereplication of peptidic natural products through database search of mass spectra. *Nat Chem Biol* 13(1): 30-37. https://doi.org/10.1038/nchembio.2219

Mueller LO, Borstein SR, Tague ED, Dearth SP, Castro HF, Campagna SR, Bailey JK, Schweitzer JA 2020. Populations of *Populus angustifolia* have evolved distinct metabolic profiles that influence their surrounding soil. *Plant Soil* 448: 399-411. https://doi.org/10.1007/s11104-019-04405-2

Nacke H, Goldmann K, Schöning I, Pfeiffer B, Kaiser K, Villamizar GAC, Schrumpf M, Buscot F, Daniel R, Wubet T 2016. Fine spatial scale variation of soil microbial communities under European beech and Norway spruce. *Front Microbiol* 7: 2067. https://doi.org/10.3389/fmicb.2016.02067

Naveh Z 2000. What is holistic landscape ecology? A conceptual introduction. *Landsc Urban Plan* 50(1-3): 7-26. https://doi.org/10.1016/S0169-2046(00)00077-3

Nothias LF, Petras D, Schmid R, Dührkop K, Rainer J, Sarvepalli A, Protsyuk I, Ernst M, Tsugawa H, Fleischauer M, Aicheler F, Aksenov AA, Alka O, Allard PM, Barsch A, Cachet X, Caraballo-Rodriguez AM, Da Silva RR, Dang T, Garg N, Gauglitz JM, Gurevich A, Isaac G, Jarmusch AK, Kameník Z, Kang KB, Kessler N, Koester I, Korf A, Le Gouellec A, Ludwig M, Martin H C, McCall LI, McSayles J, Meyer SW, Mohimani H, Morsy M, Moyne O, Neumann S, Neuweger H, Nguyen NH, Nothias-Esposito M, Paolini J, Phelan VV, Pluskal T, Quinn RA, Rogers S, Shrestha B, Tripathi A, van der Hooft JJJ, Vargas F, Weldon KC, Witting M, Yang H, Zhang Z, Zubeil F, Kohlbacher O, Böcker S, Alexandrov T, Bandeira N, Wang M, Dorrestein PC 2020. Feature-based molecular networking in the GNPS analysis environment. *Nat Methods* 17(9): 905-908. https://doi.org/10.1038/s41592-020-0933-6

Obermann A, Bastin S, Belamari S, Conte D, Gaertner MA, Li L, Ahrens B 2018. Mistral and Tramontane wind speed and wind direction patterns in regional climate simulations. *Clim Dyn* 51: 1059-1076. https://doi.org/10.1007/s00382-016-3053-3

Oddou-Muratorio S, Petit-Cailleux C, Journé V, Lingrand M, Magdalou JA, Hurson C, Garrigue J, Davi H, Magnanou E 2021. Crown defoliation decreases reproduction and wood growth in a marginal European beech population. *Ann Bot* 128(2): 193-204. https://doi.org/10.1093/aob/mcab054

Oksanen J, Simpson G, Blanchet F, Kindt R, Legendre P, Minchin P, O'Hara R, Solymos P, Stevens M, Szoecs E, Wagner H, Barbour M, Bedward M, Bolker B, Borcard D, Carvalho G, Chirico M, De Caceres M, Durand S, Evangelista H, FitzJohn R, Friendly M, Furneaux B, Hannigan G, Hill M, Lahti L, McGlinn D, Ouellette M, Ribeiro Cunha E, Smith T, Stier A, Ter Braak C, Weedon J 2022. vegan: Community Ecology Package. R package version 2.6-4, https://vegandevs.github.io/vegan

Olsson PA 2006. Signature fatty acids provide tools for determination of the distribution and interactions of mycorrhizal fungi in soil. *FEMS Microbiol Ecol* 29(4): 303-310. https://doi.org/10.1111/j.1574-6941.1999.tb00621.x

Otasek D, Morris JH, Bouças J, Pico AR, Demchak B 2019. Cytoscape Automation: empowering workflow-based network analysis. *Genome Biol* 20(1): 185. https://doi.org/10.1186/s13059-019-1758-4

Parks SC, Nguyen S, Boulanger MJ, Dillman AR 2022. The FAR protein family of parasitic nematodes. *PLoS Pathog* 18: e1010424. https://doi.org/10.1371/journal.ppat.1010424

Patti GJ, Yanes O, Siuzdak G 2012. Innovation: Metabolomics: the apogee of the omics trilogy. *Nat Rev Mol Cell Biol* 13(4): 263-269

Peñuelas J, Sardans J, Filella I, Estiarte M, Llusià J, Ogaya R, Carnicer J, Bartrons M, Rivas-Ubach A, Grau O, Peguero G, Margalef O, Pla-Rabés S, Stefanescu C, Asensio D, Preece C, Liu L, Verger A, Barbeta A, Guerrieri R, Peaucelle M, Marañón-Jiménez S, Bórnez-Mejías K, Mu Z, Descals A, Castellanos A, Terradas J 2017. Impacts of global change on Mediterranean forests and their services. Forests 8(12): 463. https://doi.org/10.3390/f8120463

Petrén H, Köllner TG, Junker RR 2023. Quantifying chemodiversity considering biochemical and structural properties of compounds with the R package chemodiv. *New Phytol* 237(6): 2478-2492. https://doi.org/10.1111/nph.18685

Pétriacq P, Williams A, Cotton A, McFarlane AE, Rolfe SA, Ton J 2017. Metabolite profiling of non-sterile rhizosphere soil. *Plant J* 92(1): 147-162. https://doi.org/10.1111/tpj.13639

Pluskal T, Castillo S, Villar-Briones A, Orešič M 2010. MZmine 2: Modular framework for processing, visualizing, and analyzing mass spectrometry-based molecular profile data. *BMC Bioinformatics* 11: 395. https://doi.org/10.1186/1471-2105-11-395

Pott R 2018. Changes in the landscape and vegetation under the influence of prehistoric and historic man in Central Europe. *In* Geographical changes in vegetation and plant functional types. Geobotany Studies. Greller A, Fujiwara K, Pedrotti F eds, Springer, Cham, Switzerland, 359 p.

Quan W, Wang A, Li C, Xie L 2022. Allelopathic potential and allelochemical composition in different soil layers of *Rhododendron delavayi* forest, southwest China. *Front Ecol Evol* 10: 963116. https://doi.org/10.3389/fevo.2022.963116

Risser PG 1987. Landscape ecology: State of the art. *In* Ecological studies: Landscape heterogeneity and disturbance. Turner M ed, Springer, New-York, NY, 240 p.

Rivest D, Paquette A, Shipley B, Reich PB, Messier C 2015. Tree communities rapidly alter soil microbial resistance and resilience to drought. *Funct Ecol* 29(4): 570-578. https://doi.org/10.1111/1365-2435.12364

Rodrigues AMS, Lebaron P, Downs CA, Stien D 2021. Optimization method for quantification of sunscreen organic ultraviolet filters in coastal sands. *J Sep Sci* 44(18): 3338-3347. https://doi.org/10.1002/jssc.202100400

Rogozhin EA, Sadykova VS, Baranova AA, Vasilchenko AS, Lushpa VA, Mineev KS, Georgieva ML, Kul'ko AB, Krasheninnikov ME, Lyundup AV, Vasilchenko AV, Andreev YA 2018. A novel lipopeptaibol emericellipsin a with antimicrobial and antitumor activity produced by the extremophilic fungus *Emericellopsis alkalina*. Molecules 23(11): 2785. https://doi.org/10.3390/molecules23112785

Ruess L, Chamberlain PM 2010. The fat that matters: Soil food web analysis using fatty acids and their carbon stable isotope signature. *Soil Biol Biochem* 42(11): 1898-1910. https://doi.org/10.1016/j.soilbio.2010.07.020

Ruess L, Häggblom MMH, Garcõ EJ, Dighton J 2002. Fatty acids of fungi and nematodes - possible biomarkers in the soil food chain? *Soil Biol Biochem* 34(6): 745-756. https://doi.org/https://doi.org/10.1016/S0038-0717(01)00231-0

Sarabia LD, Boughton BA, Rupasinghe T, Callahan DL, Hill CB, Roessner U 2020. Comparative spatial lipidomics analysis reveals cellular lipid remodelling in different developmental zones of barley roots in response to salinity. *Plant Cell Environ* 43(2): 327-343. https://doi.org/10.1111/pce.13653

Semchenko M, Barry KE, de Vries FT, Mommer L, Moora M, Maciá-Vicente JG 2022. Deciphering the role of specialist and generalist plant–microbial interactions as drivers of plant–soil feedback. *New Phytol* 234(6): 1929-1944. https://doi.org/10.1111/nph.18118

Servat E, Servant J 1972. La carte pédologique au 1/100 000. Feuille de Perpignan-Argeles-Sur-Mer. *Bull Ass Fr étude Quaternaire* 9: 219-220

Shannon P, Markiel A, Ozier O, Baliga NS, Wang JT, Ramage D, Amin N, Schwikowski

B, Ideker T 2003. Cytoscape: a software environment for integrated models of biomolecular interaction networks. *Genome Res* 13(11): 2498-2504. https://doi.org/10.1101/gr.1239303

Shen H, Yan W, Yang X, He X, Wang X, Zhang Y, Wang B, Xia Q 2020. Co-occurrence network analyses of rhizosphere soil microbial PLFAs and metabolites over continuous cropping seasons in tobacco. *Plant Soil* 452: 119-135. https://doi.org/10.1007/s11104-020-04560-x

Song Y, Yao S, Li X, Wang T, Jiang X, Bolan N, Warren CR, Northen TR, Chang SX 2024. Soil metabolomics: Deciphering underground metabolic webs in terrestrial ecosystems. *EEH* 3(2): 227-237. https://doi.org/10.1016/j.eehl.2024.03.001

Staszel-Szlachta K, Lasota J, Szlachta A, Błońska E 2024. The impact of root systems and their exudates in different tree species on soil properties and microorganisms in a temperate forest ecosystem. *BMC Plant Biol* 24: 45. https://doi.org/10.1186/s12870-024-04724-2

Stien D, Clergeaud F, Rodrigues AMS, Lebaron K, Pillot R, Romans P, Fagervold S, Lebaron P 2019. Metabolomics reveal that octocrylene accumulates in Pocillopora damicornis tissues as fatty acid conjugates and triggers coral cell mitochondrial dysfunction. *Anal Chem* 91: 990-995. https://doi.org/10.1021/acs.analchem.8b04187

Stringlis IA, De Jonge R, Pieterse CMJ 2019. The age of coumarins in plant-microbe interactions. *Plant Cell Physiol* 60(7): 1405-1419. https://doi.org/10.1093/pcp/pcz076

Tedersoo L, Bahram M, Cajthaml T, Põlme S, Hiiesalu I, Anslan S, Harend H, Buegger F, Pritsch K, Koricheva J, Abarenkov K 2016. Tree diversity and species identity effects on soil fungi, protists and animals are context dependent. *ISME Journal* 10: 346-362. https://doi.org/10.1038/ismej.2015.116

Truchy A, Göthe E, Angeler DG, Ecke F, Sponseller RA, Bundschuh M, Johnson RK, McKie BG 2019. Partitioning spatial, environmental, and community drivers of ecosystem functioning. *Landsc Ecol* 34: 2371-2384. https://doi.org/10.1007/s10980-019-00894-9

Tyc O, Song C, Dickschat JS, Vos M, Garbeva P 2017. The ecological role of volatile and soluble secondary metabolites produced by soil bacteria. *Trends Microbiol* 25(4): 280-292. https://doi.org/10.1016/j.tim.2016.12.002

Urbanová M, Šnajdr J, Baldrian P 2015. Composition of fungal and bacterial communities in forest litter and soil is largely determined by dominant trees. *Soil Biol Biochem* 84: 53-64. https://doi.org/10.1016/j.soilbio.2015.02.011

Van Eetvelde V, Aagaard Christensen A 2023. Theories in landscape ecology. An overview of theoretical contributions merging spatial, ecological and social logics in the study of cultural landscapes. *Landsc Ecol* 38: 4033-4064. https://doi.org/10.1007/s10980-023-01736-5

van Tilburg AY, Warmer P, van Heel AJ, Sauer U, Kuipers OP 2022. Membrane composition and organization of Bacillus subtilis 168 and its genome-reduced derivative miniBacillus PG10. *Microb Biotechnol* 15(5): 1633-1651. https://doi.org/10.1111/1751-7915.13978

Vandekerkhove K, Vanhellemont M, Vrška T, Meyer P, Tabaku V, Thomaes A, Leyman A, De Keersmaeker L, Verheyen K 2018. Very large trees in a lowland old-growth beech (*Fagus sylvatica* L.) forest: Density, size, growth and spatial patterns in comparison to reference sites in Europe. *For Ecol Manage* 417: 1-17. https://doi.org/10.1016/j.foreco.2018.02.033

Voloscuk I, Pichler V, Pichlerova M 2013. The primeval beech forests of the Carpathians and ancient beech forests of Germany: joint natural heritage of Europe. *Folia Oecologia* 40: 295-303

Walker TWN, Alexander JM, Allard PM, Baines O, Baldy V, Bardgett RD, Capdevila P, Coley PD, David B, Defossez E, Endara MJ, Ernst M, Fernandez C, Forrister D, Gargallo-Garriga A, Jassey VEJ, Marr S, Neumann S, Pellissier L, Peñuelas J, Peters K, Rasmann S, Roessner U, Sardans J, Schrodt F, Schuman MC, Soule A, Uthe H, Weckwerth W, Wolfender

JL, van Dam NM, Salguero-Gómez R (2022) Functional Traits 2.0: The power of the metabolome for ecology. *J Ecol* 110(1): 4-20. https://doi.org/10.1111/1365-2745.13826

Wang CM, Chen HT, Li TC, et al (2014) The role of pentacyclic triterpenoids in the allelopathic effects of Alstonia scholaris. *J Chem Ecol* 40: 90-98. https://doi.org/10.1007/s10886-013-0376-y

Wang M, Carver JJ, Phelan V V., Weng JH, Jhan YL, Lin SX, Chou CH 2016. Sharing and community curation of mass spectrometry data with Global Natural Products Social Molecular Networking. *Nat Biotechnol* 34(1): 828-837. https://doi.org/10.1038/nbt.3597

Wardle DA, Bardgett RD, Klironomos JN, Setälä H, van der Putten WH, Wall DH 2004. Ecological linkages between aboveground and belowground biota. *Science* 304(5677): 1629-1633. https://doi.org/10.1126/science.1094875

Whittaker RH 1960. Vegetation of the Siskiyou Mountains. *Ecol Monogr* 30(3): 279-338. https://doi.org/10.2307/1943563

Whittaker RJ, Willis KJ, Field R, Whittaker RJ 2001. Scale and species richness: towards a general, hierarchical theory of species diversity. *J Biogeogr* 28(4): 453-470. https://doi.org/10.1046/j.1365-2699.2001.00563.x

Willers C, Jansen van Rensburg PJ, Claassens S 2016. Can a metabolomics-based approach be used as alternative to analyse fatty acid methyl esters from soil microbial communities? *Soil Biol Biochem* 103: 417-428. https://doi.org/10.1016/j.soilbio.2016.09.021.

Withers E, Hill PW, Chadwick DR, Jones DL 2020. Use of untargeted metabolomics for assessing soil quality and microbial function. *Soil Biol Biochem* 143: 107758. https://doi.org/10.1016/j.soilbio.2020.107758

Wong-Bajracharya J, Castañeda-Gómez L, Plett KL, Anderson IC. Carrillo Y, Plett JM 2020. Untangling the effect of roots and mutualistic ectomycorrhizal fungi on soil metabolite profiles under ambient and elevated carbon dioxide. *Soil Biol Biochem* 151: 108021. https://doi.org/10.1016/j.soilbio.2020.108021

Wu J 2013. Key concepts and research topics in landscape ecology revisited: 30 years after the Allerton Park workshop. *Landsc Ecol* 28: 1-11. https://doi.org/10.1007/s10980-012-9836-y

Wu J, Hobbs R 2002. Key issues and research priorities in landscape ecology: An idiosyncratic synthesis. *Landsc Ecol* 17: 355-365

Yao J, Huang J, Zang R 2023. Alpha and beta diversity jointly drive the aboveground biomass in temperate and tropical forests. *Ecol Evol* 13(9): e10487. https://doi.org/10.1002/ece3.10487

Zeller L, Baumann C, Gonin P, Heidrich L, Keye C, Konrad F, Larrieu L, Meyer P, Sennhenn-Reulen H, Müller J, Schall P, Ammer C 2022. Index of biodiversity potential (IBP) versus direct species monitoring in temperate forests. *Ecol Indic* 136: 108692. https://doi.org/10.1016/j.ecolind.2022.108692

Zeng T, Liu Z, Liu H, He W, Tang X, Xie L, Wu R 2019. Exploring chemical and biological space of terpenoids. *J Chem Inf Model* 59(9): 3667-3678. https://doi.org/10.1021/acs.jcim.9b00443

Zhou G, Long F, Zu L, Jarvie S, Peng Y, Zang L, Chen D, Zhang G, Sui M, He Y, Liu Q 2024. Stand spatial structure and microbial diversity are key drivers of soil multifunctionality during secondary succession in degraded karst forests. *Sci Total Environ* 937: 173504. https://doi.org/10.1016/j.scitotenv.2024.173504

Received on 21/11/2024
Accepted on 19/05/2025

Supplementary Materials

pairs				Df	SumsOfSqs	F.Model	R2	p.value	p.adjusted	sig
1	G	vs	Y	1	0.23631893	10.189817	0.3890755	0.001	0.01	*
2	G	vs	V	1	0.22686030	10.685385	0.5165669	0.003	0.03	.
3	G	vs	R	1	0.29715382	16.536807	0.6231649	0.002	0.02	.
4	G	vs	B	1	0.23319618	11.600792	0.6236719	0.012	0.12	
5	Y	vs	V	1	0.09142504	3.672592	0.1866857	0.001	0.01	*
6	Y	vs	R	1	0.14241428	6.231117	0.2802881	0.001	0.01	*
7	Y	vs	B	1	0.17836314	7.097286	0.3531465	0.004	0.04	.
8	V	vs	R	1	0.14626312	7.068324	0.4141194	0.003	0.03	.
9	V	vs	B	1	0.21401589	8.920120	0.5603048	0.014	0.14	
10	R	vs	B	1	0.06369333	3.294543	0.3200281	0.013	0.13	

Table S1.- Effect of soil subgroup on the structure of chemical communities (Hellinger-transformed relative abundances), pairwise multi-level comparisons. Permutational multivariate analysis of variance based on Bray-Curtis distance matrix (PERMANOVA: adonis function with 999 permutations)

Feature	Parent mass	ATTRIBUTE_SampleType	GNPSGROUP: Green	GNPSGROUP: Yellow	GNPSGROUP: Violet	GNPSGROUP: Red	GNPSGROUP: Blue
1	145.1012	Yellow; Blue; Violet; Green; Red	680270.4273	358297.9537	648440.6157	609459.8318	9.77E+07
2	173.1325	Yellow; Blue; Violet; Green; Red	752197.5541	600091.8327	880745.6345	576000.9889	6.26E+08
3	187.1482	Yellow; Blue; Violet; Green; Red	1162846.052	402758.2077	993984.4905	474049.67	1.02E+08
4	191.1431	Yellow; Blue; Violet; Green; Red	806855.4508	697952.0656	898487.51	691089.6918	1.27E+08
5	191.1795	Yellow; Blue; Violet; Green; Red	7.23E+07	3.78E+07	7.88E+07	2.48E+07	2.22E+07
6	201.1274	Yellow; Blue; Violet; Green; Red	206528.8424	406757.1253	507061.8465	1611427.971	3.97E+08
7	215.1431	Yellow; Blue; Violet; Green; Red	1438459.511	2.28E+07	5.20E+07	1.48E+07	7389257.29
8	215.1431	Yellow; Blue; Violet; Green; Red	1564428.107	3.09E+07	7.18E+07	1.51E+07	1.27E+07
9	215.1431	Yellow; Blue; Violet; Green; Red	566172.6708	8323945.02	1.93E+07	5842043.602	5505119.153
10	217.1224	Yellow; Blue; Violet; Green; Red	214358.2569	215631.1128	248996.9077	769450.4833	7.00E+07
11	219.138	Yellow; Blue; Violet; Green; Red	621348.1013	540606.1258	647403.6593	652507.1186	1.44E+09
12	231.2108	Yellow; Blue; Violet; Green; Red	122216.8794	1.54E+07	288439.0199	242047.7512	207304.2856
13	233.1536	Yellow; Blue; Violet; Green; Red	1286721.204	939832.9695	1911029.998	1355716.624	3.35E+08
14	233.1536	Yellow; Blue; Violet; Green; Red	708946.0495	852110.5803	1540335.621	1689644.962	1.01E+08
15	233.1536	Yellow; Blue; Violet; Green; Red	1463789.45	8327809.693	2.18E+07	7852651.671	9774867.262
16	245.0809	Yellow; Blue; Violet; Green; Red	6104951.509	5.41E+07	3055507.177	342547.8963	6264682.931
17	247.133	Yellow; Blue; Violet; Green; Red	561145.2507	775822.9329	691711.6882	1732495.186	2.15E+09

18	251.1642	Yellow; Blue; Violet; Green; Red	1109533.903	731805.0585	1015544.31	2731307.346	1.57E+08
19	256.2635	Yellow; Blue; Violet; Green; Red	1.05E+08	9.21E+07	1.25E+08	1.45E+08	8.04E+07
20	263.237	Yellow; Blue; Violet; Green; Red	1.64E+07	1.82E+07	4.52E+07	1.86E+07	8672645.039
21	263.237	Yellow; Blue; Violet; Green; Red	6508479.776	7042087.335	5.45E+07	4186108.471	1589471.107
22	265.1433	Yellow; Blue; Violet; Green; Red	449755.1594	162625.3703	284170.9609	291448.7157	1.76E+09
23	274.2741	Yellow; Blue; Violet; Green; Red	3.92E+08	3.99E+08	4.00E+08	4.30E+08	4.43E+08
24	275.2007	Yellow; Blue; Violet; Green; Red	1785606.751	1.95E+07	2389399.586	1322561.944	3401527.691
25	279.232	Yellow; Blue; Violet; Green; Red	1.17E+07	2.55E+07	4.00E+07	6.41E+07	9.34E+07
26	281.138	Yellow; Blue; Violet; Green; Red	159802.4315	117830.8413	434197.8275	502067.2813	5.11E+07
27	281.1382	Yellow; Blue; Violet; Green; Red	0	2187214.025	1.27E+07	2.72E+07	4917771.895
28	281.2476	Yellow; Blue; Violet; Green; Red	282881.3271	470591.6592	3.98E+07	369876.1138	497206.9931
29	282.2793	Yellow; Blue; Violet; Green; Red	2.35E+08	2.19E+08	6.21E+08	6.72E+08	6.73E+08
30	287.0915	Yellow; Blue; Violet; Green; Red	5894092.916	5.26E+07	2827246.429	362484.3964	6205372.1
31	287.1255	Yellow; Blue; Violet; Green; Red	20423.05684	1395.557833	837.7586095	22985.23098	7.66E+08
32	290.1024	Yellow; Blue; Violet; Green; Red	987.2885988	641.1372856	0	2.14E+07	108512.711
33	290.269	Yellow; Blue; Violet; Green; Red	2.38E+07	2.52E+07	2.66E+07	5.63E+07	3.89E+07
34	291.0653	Yellow; Blue; Violet; Green; Red	3929132.443	8.93E+07	7.22E+07	1.68E+08	1.58E+08
35	295.1281	Yellow; Blue; Violet; Green; Red	0	895.6403328	0	0	4.50E+07
36	299.2582	Yellow; Blue; Violet; Green; Red	2225375.603	1829566.408	2.70E+07	890567.2403	198552.4737

37	299.2582	Yellow; Blue; Violet; Green; Red	6.07E+07	2.20E+07	8.33E+07	1.35E+07	3453777.442
38	301.2163	Yellow; Blue; Violet; Green; Red	1199560.959	1.52E+07	2624345.971	4877177.123	8.18E+07
39	309.0758	Yellow; Blue; Violet; Green; Red	3.01E+07	5.87E+08	4.88E+08	1.04E+09	9.75E+08
40	309.0759	Yellow; Blue; Violet; Green; Red	717408.2395	1.50E+07	9341372.444	7.93E+07	7.05E+07
41	309.0759	Yellow; Blue; Violet; Green; Red	32932.65803	1.10E+07	1060709.401	1.68E+07	1.37E+07
42	311.2582	Yellow; Blue; Violet; Green; Red	3.48E+07	1.77E+07	1.01E+08	1.21E+07	3705143.334
43	313.2163	Yellow; Blue; Violet; Green; Red	200659.5035	1.42E+07	859528.2842	1.64E+07	2.02E+08
44	313.2738	Yellow; Blue; Violet; Green; Red	4.97E+07	1.92E+07	5.68E+07	1.64E+07	1.01E+07
45	313.2738	Yellow; Blue; Violet; Green; Red	1.05E+07	8184019.589	3.36E+07	5408821.586	2375642.532
46	313.2889	Yellow; Blue; Violet; Green; Red	5172.945859	2.71E+07	97813.6399	22928.65394	34476.7251
47	315.232	Yellow; Blue; Violet; Green; Red	6.40E+07	4.83E+07	6.14E+07	9.43E+07	2.10E+08
48	318.3004	Yellow; Blue; Violet; Green; Red	6.16E+07	6.36E+07	1.16E+08	1.35E+08	7.27E+07
49	321.3154	Yellow; Blue; Violet; Green; Red	2.62E+08	2.29E+08	1.64E+08	2.63E+08	3.57E+08
50	327.1228	Yellow; Blue; Violet; Green; Red	7312263.222	8.04E+07	1.19E+07	2618020.435	5895468.165
51	327.1228	Yellow; Blue; Violet; Green; Red	9736221.955	6.59E+07	1.14E+07	2522620.658	5639990.578
52	329.2687	Yellow; Blue; Violet; Green; Red	2.47E+07	1.11E+07	6.94E+07	7296916.266	3658319.066
53	331.2997	Yellow; Blue; Violet; Green; Red	136211.8794	6.62E+07	252789.5071	53348.8883	16934.29127
54	337.2738	Yellow; Blue; Violet; Green; Red	2.80E+07	2.99E+07	8.61E+07	3.18E+07	1.39E+07
55	338.3419	Yellow; Blue; Violet; Green; Red	3.21E+07	3.37E+07	8.30E+07	8.36E+07	1.04E+08

56	339.2895	Yellow; Blue; Violet; Green; Red	7.58E+07	4.24E+07	1.03E+08	1.63E+07	1.49E+07
57	339.3259	Yellow; Blue; Violet; Green; Red	5.37E+08	4.78E+08	3.44E+08	5.40E+08	7.36E+08
58	343.248	Yellow; Blue; Violet; Green; Red	2.84E+07	2.20E+07	4.77E+07	2.93E+07	2.44E+07
59	346.2377	Yellow; Blue; Violet; Green; Red	3226932.52	2.87E+07	5.61E+07	7.60E+07	1.27E+08
60	349.3467	Yellow; Blue; Violet; Green; Red	1.49E+08	1.28E+08	8.44E+07	1.21E+08	1.69E+08
61	351.2531	Yellow; Blue; Violet; Green; Red	1179581.712	1.01E+07	3.48E+07	9.32E+07	3.36E+07
62	353.3052	Yellow; Blue; Violet; Green; Red	4.87E+07	1.68E+07	4.43E+07	1.18E+07	6685983.362
63	355.2455	Yellow; Blue; Violet; Green; Red	1.22E+07	2.96E+07	3.60E+07	8.53E+07	1.57E+08
64	355.2843	Yellow; Blue; Violet; Green; Red	2.55E+07	2.36E+07	6.46E+07	2.88E+07	1.70E+07
65	357.3	Yellow; Blue; Violet; Green; Red	6.89E+07	3.87E+07	8.74E+07	1.12E+07	1.33E+07
66	367.3572	Yellow; Blue; Violet; Green; Red	3.67E+08	3.17E+08	2.14E+08	3.03E+08	4.06E+08
67	369.2613	Yellow; Blue; Violet; Green; Red	9448409.645	1.36E+07	3.54E+07	1.88E+07	9403528.516
68	371.3157	Yellow; Blue; Violet; Green; Red	5.48E+07	1.68E+07	4.74E+07	9450499.552	3378986.207
69	371.3157	Yellow; Blue; Violet; Green; Red	1.78E+08	1.65E+08	1.06E+08	2.13E+08	2.92E+08
70	372.2533	Yellow; Blue; Violet; Green; Red	109369.2732	4094022.743	1.06E+07	9398428.242	4.98E+07
71	374.1598	Blue; Red	0	0	0	2.17E+07	87376.87971
72	377.3202	Yellow; Blue; Violet; Green; Red	2.18E+07	3.24E+07	1.95E+07	7.75E+07	4.50E+07
73	377.3203	Yellow; Blue; Violet; Green; Red	3.65E+07	3.66E+07	7.22E+07	7.37E+07	4.90E+07
74	377.3204	Yellow; Blue; Violet; Green; Red	3.63E+07	2.65E+07	7.12E+07	6.57E+07	5.26E+07

75	377.3204	Yellow; Blue; Violet; Green; Red	1.49E+08	1.75E+08	2.97E+08	2.98E+08	2.08E+08
76	377.3204	Yellow; Blue; Violet; Green; Red	2.61E+07	3.25E+07	5.99E+07	5.89E+07	4.87E+07
77	377.3205	Yellow; Blue; Violet; Green; Red	1.62E+07	1.65E+07	6.58E+07	1.83E+07	1.35E+07
78	383.0763	Yellow; Blue; Violet; Green; Red	4471.826483	1.13E+07	30514.21645	4842126.554	4365026.25
79	383.3156	Yellow; Blue; Violet; Green; Red	3.41E+07	2.06E+07	2.34E+07	2.33E+07	4.49E+07
80	385.201	Yellow; Blue; Violet; Green; Red	89199.20604	58310.86055	1332979.371	3.37E+07	4.65E+07
81	385.3313	Yellow; Blue; Violet; Green; Red	6.25E+07	5.14E+07	3.43E+07	5.46E+07	8.25E+07
82	385.3314	Yellow; Blue; Violet; Green; Red	4.75E+07	3.99E+07	1.91E+07	4.36E+07	6.42E+07
83	386.3994	Yellow; Blue; Violet; Green; Red	9105971.366	1.94E+07	7859364.65	1.39E+08	3.42E+07
84	393.3153	Yellow; Blue; Violet; Green; Red	3.92E+08	3.89E+08	7.54E+08	4.51E+08	1.87E+08
85	393.3517	Yellow; Blue; Violet; Green; Red	1.48E+08	7.59E+07	1.30E+08	3.07E+07	3.77E+07
86	394.3466	Yellow; Blue; Violet; Green; Red	23617.10113	25446.26969	58667.52219	2.96E+07	59794.71332
87	395.331	Yellow; Blue; Violet; Green; Red	9.23E+07	1.08E+08	3.57E+08	8.14E+07	3.65E+07
88	395.3673	Yellow; Blue; Violet; Green; Red	3.78E+07	3.34E+07	4.68E+07	2.47E+07	1.48E+07
89	395.3674	Yellow; Blue; Violet; Green; Red	9.28E+07	6.65E+07	9.31E+07	3.82E+07	2.32E+07
90	396.1418	Blue; Red	0	0	0	5.26E+07	371561.3118
91	397.3831	Yellow; Blue; Violet; Green; Red	1.29E+08	1.08E+08	1.41E+08	1.02E+08	6.58E+07
92	399.3106	Yellow; Blue; Violet; Green; Red	3.61E+07	4.38E+07	3.54E+07	6.17E+07	1.02E+08
93	399.3258	Yellow; Blue; Violet; Green; Red	1.06E+07	1.28E+07	2.22E+07	1.90E+07	6.43E+07

94	399.347	Yellow; Blue; Violet; Green; Red	1.86E+08	1.42E+08	9.50E+07	1.52E+08	1.93E+08
95	403.154	Yellow; Blue; Violet; Green; Red	29358.01551	7756281.183	679754.6191	1060939.074	4.86E+07
96	404.1705	Yellow; Blue; Violet; Green; Red	5391288.936	3.26E+07	1811520.707	147519.2248	3817581.313
97	405.1332	Yellow; Blue; Violet; Green; Red	7137.446592	1.33E+07	529206.5731	724288.0216	532368.0764
98	405.1698	Yellow; Blue; Violet; Green; Red	42169.74208	2025225.629	396675.7467	231636.7744	1.22E+08
99	405.3516	Yellow; Blue; Violet; Green; Red	1827332.04	3.87E+07	1.94E+07	4.39E+07	1.25E+07
100	405.3518	Yellow; Blue; Violet; Green; Red	4618880.717	1.56E+07	4.45E+07	3.73E+07	1.01E+07
101	405.3518	Yellow; Blue; Violet; Green; Red	1.15E+07	4.14E+08	8.33E+08	4.67E+08	5.54E+07
102	407.1854	Yellow; Blue; Violet; Green; Red	9196.010713	49138.17147	2421528.249	15528.02228	2.25E+07
103	407.1855	Yellow; Blue; Violet; Green; Red	21646.53134	102124.5926	727285.1472	4376.523813	4.28E+07
104	407.352	Yellow; Blue; Violet; Green; Red	8744582.773	7259798.697	9136254.378	1.80E+07	7513738.748
105	407.3673	Yellow; Blue; Violet; Green; Red	2.24E+07	1.19E+07	5.38E+07	1.52E+07	1.96E+07
106	407.3674	Yellow; Blue; Violet; Green; Red	3289220.439	1.87E+07	3.52E+07	1.53E+07	2.52E+07
107	407.3675	Yellow; Blue; Violet; Green; Red	1.20E+07	4.16E+07	7.30E+07	6.96E+07	4.52E+07
108	409.126	Yellow; Blue; Violet; Green; Red	8078398.864	4.69E+07	2814305.173	329672.7429	5887868.264
109	409.3466	Yellow; Blue; Violet; Green; Red	2.44E+07	1.78E+07	2.74E+07	1.56E+07	1.84E+07
110	409.3466	Yellow; Blue; Violet; Green; Red	8.67E+07	8.90E+07	1.35E+08	5.17E+07	1.95E+07
111	409.383	Yellow; Blue; Violet; Green; Red	1947088.061	2.46E+07	5.67E+07	2.70E+07	1.18E+07
112	409.383	Yellow; Blue; Violet; Green; Red	3940201.053	3961501.738	6796022.773	4.29E+07	1.82E+07

113	411.1075	Yellow; Blue; Violet; Green; Red	7491.216051	5.66E+07	313789.9087	4.51E+07	4.05E+07
114	411.1804	Yellow; Blue; Violet; Green; Red	24092.81512	33301.30053	3.52E+07	7.11E+07	4.26E+07
115	411.3258	Yellow; Blue; Violet; Green; Red	2256289.109	2.62E+07	6116575.133	1.10E+07	6613532.726
116	411.3622	Yellow; Blue; Violet; Green; Red	2.88E+08	1.89E+08	2.64E+08	9.35E+07	6.76E+07
117	411.3622	Yellow; Blue; Violet; Green; Red	3.70E+07	2.49E+07	1.95E+07	2.41E+07	1.82E+07
118	411.3622	Yellow; Blue; Violet; Green; Red	1.08E+08	1.33E+08	1.54E+08	1.18E+08	6.69E+07
119	411.3622	Yellow; Blue; Violet; Green; Red	9.18E+07	7.48E+07	1.16E+08	6.22E+07	2.94E+07
120	411.3622	Yellow; Blue; Violet; Green; Red	2.62E+08	9.10E+07	2.31E+08	2.37E+07	2.11E+07
121	411.3987	Yellow; Blue; Violet; Green; Red	549441.2299	1.36E+07	2.64E+08	2.06E+08	1467793
122	413.3415	Yellow; Blue; Violet; Green; Red	3605321.173	6144663.558	1.02E+07	3.11E+07	6.75E+07
123	413.3626	Yellow; Blue; Violet; Green; Red	9.33E+07	5.50E+07	5.65E+07	7.77E+07	9.50E+07
124	413.3627	Yellow; Blue; Violet; Green; Red	4.51E+08	4.04E+08	3.35E+08	5.93E+08	7.52E+08
125	413.3779	Yellow; Blue; Violet; Green; Red	5.19E+08	4.14E+08	6.50E+08	2.32E+08	9.45E+07
126	413.378	Yellow; Blue; Violet; Green; Red	5.06E+07	4.02E+07	4.66E+07	2.90E+07	2.45E+07
127	414.3579	Yellow; Blue; Violet; Green; Red	7.39E+07	7.60E+07	2.34E+07	1.44E+07	1.43E+07
128	419.3368	Yellow; Blue; Violet; Green; Red	2.98E+07	1.88E+07	1.97E+07	1.73E+07	4.05E+07
129	421.3467	Yellow; Blue; Violet; Green; Red	5898260.826	2.67E+07	4.78E+07	3.63E+07	1.43E+07
130	423.3622	Yellow; Blue; Violet; Green; Red	1.01E+07	4.91E+07	7.77E+07	6.73E+07	1.92E+07
131	423.3623	Yellow; Blue; Violet; Green; Red	7.21E+07	1.50E+09	2.94E+09	1.68E+09	3.00E+08

132	423.3624	Yellow; Blue; Violet; Green; Red	4.41E+07	3.76E+07	5.84E+07	2.19E+08	6.99E+08
133	423.3624	Yellow; Blue; Violet; Green; Red	1.57E+07	1.47E+08	4.27E+07	1.69E+08	8357429.169
134	423.3624	Yellow; Blue; Violet; Green; Red	1.26E+07	3.06E+07	2.86E+07	4.11E+07	1.77E+07
135	423.3624	Yellow; Blue; Violet; Green; Red	1.79E+07	1.45E+08	2.67E+08	1.96E+08	1.86E+07
136	423.3625	Yellow; Blue; Violet; Green; Red	1.76E+07	1.45E+07	2.03E+07	7.81E+07	1.18E+08
137	423.3626	Yellow; Blue; Violet; Green; Red	4.97E+07	2.06E+07	1.63E+07	1.08E+07	1.47E+07
138	425.3416	Yellow; Blue; Violet; Green; Red	2.05E+07	1.95E+07	2.77E+07	1.85E+07	1.61E+07
139	425.3416	Yellow; Blue; Violet; Green; Red	6072724.651	1.28E+07	5855939.737	1.03E+07	9782270.245
140	425.3627	Yellow; Blue; Violet; Green; Red	8396755.61	1.05E+07	1.88E+07	2.61E+07	8566597.068
141	425.3778	Yellow; Blue; Violet; Green; Red	4.58E+07	2.24E+08	3.62E+08	3.43E+08	2.40E+08
142	425.3779	Yellow; Blue; Violet; Green; Red	2.05E+07	2.12E+07	8.35E+07	3.14E+07	4.13E+07
143	425.378	Yellow; Blue; Violet; Green; Red	1.01E+07	3.25E+07	6.59E+07	1.02E+08	3.19E+07
144	425.378	Yellow; Blue; Violet; Green; Red	1.09E+07	2.79E+07	1.80E+07	1.82E+08	9.84E+07
145	427.1177	Yellow; Blue; Violet; Green; Red	2805500.994	4.09E+07	2.87E+07	8.59E+07	7.79E+07
146	427.3031	Yellow; Blue; Violet; Green; Red	1.10E+07	1.38E+07	1.22E+07	1.08E+07	3.13E+07
147	427.321	Yellow; Blue; Violet; Green; Red	9127291.003	4998710.931	6.40E+07	4483276.543	1933638.929
148	427.342	Yellow; Blue; Violet; Green; Red	1.69E+08	1.75E+08	1.35E+08	2.31E+08	3.59E+08
149	427.3569	Yellow; Blue; Violet; Green; Red	6.04E+07	2.25E+07	2.70E+07	2.29E+07	2.11E+07
150	427.3572	Yellow; Blue; Violet; Green; Red	8271431.803	5.75E+07	1.17E+08	1.00E+08	4.71E+07

151	428.2796	Yellow; Blue; Violet; Green; Red	4.36E+07	8841364.707	210676.3427	179864.5245	11413.3403
152	429.3729	Yellow; Blue; Violet; Green; Red	1.48E+08	6.58E+07	1.12E+08	4.34E+07	1.94E+07
153	429.3729	Yellow; Blue; Violet; Green; Red	4.49E+08	4.44E+08	5.08E+08	4.11E+08	2.59E+08
154	431.3521	Yellow; Blue; Violet; Green; Red	4.90E+08	1.36E+08	2.83E+08	5.13E+07	3.00E+07
155	435.3259	Yellow; Blue; Violet; Green; Red	1.56E+07	2.13E+07	3.15E+07	2.12E+07	1.27E+07
156	437.3413	Yellow; Blue; Violet; Green; Red	3915490.838	7769628.248	5227455.692	3.84E+07	6.06E+07
157	437.3414	Yellow; Blue; Violet; Green; Red	3264246.789	93530.97489	2.76E+07	289874.6364	79543.23194
158	437.3414	Yellow; Blue; Violet; Green; Red	2.09E+07	2.76E+07	4.38E+07	3.97E+07	1.64E+07
159	437.3414	Yellow; Blue; Violet; Green; Red	1.52E+08	7.32E+07	1.52E+08	3.76E+07	8.79E+07
160	437.3415	Yellow; Blue; Violet; Green; Red	6.52E+07	4949624.406	1.35E+07	2900415.161	4537036.822
161	437.3415	Yellow; Blue; Violet; Green; Red	3.36E+07	2.54E+07	1.42E+07	2.16E+07	3.36E+07
162	437.3415	Yellow; Blue; Violet; Green; Red	1.23E+08	1.22E+08	1.99E+08	7.19E+07	2.07E+07
163	437.3415	Yellow; Blue; Violet; Green; Red	8.22E+07	1.00E+07	3.64E+07	2821754.216	1820877.736
164	437.3415	Yellow; Blue; Violet; Green; Red	6.26E+07	5.22E+07	1.32E+08	9.40E+07	5.22E+07
165	437.3415	Yellow; Blue; Violet; Green; Red	1.12E+08	9338634.46	3.17E+07	1151030.717	1409807
166	437.3415	Yellow; Blue; Violet; Green; Red	5.13E+07	5859745.093	2.43E+07	2662123.411	5411460.56
167	437.3415	Yellow; Blue; Violet; Green; Red	2.19E+07	4948273.873	1.18E+07	3377040.918	2627018.187
168	437.3415	Yellow; Blue; Violet; Green; Red	2.09E+07	2.18E+07	2.76E+07	2.24E+07	3.82E+07
169	437.3415	Yellow; Blue; Violet; Green; Red	4.37E+07	8.73E+07	1.43E+08	5.57E+07	3.55E+07

170	437.3415	Yellow; Blue; Violet; Green; Red	7.04E+07	2.75E+07	3.09E+07	2.63E+07	1.20E+07
171	437.3415	Yellow; Blue; Violet; Green; Red	4.87E+07	1.17E+07	3.54E+07	1.86E+07	1.07E+07
172	437.3415	Yellow; Blue; Violet; Green; Red	1.50E+08	6.80E+07	1.23E+08	2.58E+07	1.16E+07
173	437.3416	Yellow; Blue; Violet; Green; Red	4.69E+07	6.00E+07	1.13E+08	6.59E+07	6.49E+07
174	437.3416	Yellow; Blue; Violet; Green; Red	4.60E+07	2.77E+07	5.33E+07	1.76E+07	2.33E+07
175	439.2478	Yellow; Blue; Violet; Green; Red	2744851.794	3.13E+07	1.08E+07	1906499.078	1096200.235
176	439.3209	Yellow; Blue; Violet; Green; Red	2153836.155	4.02E+07	3327323.305	5740006.962	6815018.509
177	439.3572	Yellow; Blue; Violet; Green; Red	1.41E+09	8.22E+08	1.30E+09	3.14E+08	5.68E+08
178	439.3572	Yellow; Blue; Violet; Green; Red	1.09E+07	6305294.244	2.60E+07	1.89E+07	2.04E+07
179	439.3572	Yellow; Blue; Violet; Green; Red	2.00E+07	2.81E+07	3.81E+07	7.67E+07	1.02E+08
180	439.3572	Yellow; Blue; Violet; Green; Red	4.29E+08	3.44E+08	4.47E+08	6.32E+08	5.70E+08
181	439.3573	Yellow; Blue; Violet; Green; Red	4627451.503	2.13E+07	2.86E+07	3.27E+07	1.91E+07
182	439.3573	Yellow; Blue; Violet; Green; Red	1.29E+07	2.60E+07	9405336.142	2.67E+07	1.34E+07
183	439.3573	Yellow; Blue; Violet; Green; Red	2.87E+07	2.17E+07	3.18E+07	7.12E+07	1.53E+08
184	439.3573	Yellow; Blue; Violet; Green; Red	1.18E+07	2.70E+07	8742120.502	4.03E+07	1.22E+07
185	439.3574	Yellow; Blue; Violet; Green; Red	5.04E+07	2.59E+07	4.11E+07	1.12E+08	1.19E+08
186	439.3574	Yellow; Blue; Violet; Green; Red	6.22E+07	2.06E+07	1.79E+07	4.12E+07	2.16E+07
187	441.3187	Yellow; Blue; Violet; Green; Red	4.24E+07	3.25E+07	2.70E+07	3.63E+07	7.81E+07
188	441.3364	Yellow; Blue; Violet; Green; Red	748621.3361	316859.0879	2.19E+07	150817.8367	219375.1645

189	441.3728	Yellow; Blue; Violet; Green; Red	6.51E+07	5.86E+07	8.27E+07	3.49E+08	1.02E+09
190	441.3728	Yellow; Blue; Violet; Green; Red	4352139.619	1.77E+07	2.76E+07	2.68E+07	2.76E+07
191	441.3728	Yellow; Blue; Violet; Green; Red	1.52E+07	1.91E+08	3.56E+08	2.64E+08	3.17E+07
192	441.373	Yellow; Blue; Violet; Green; Red	1.30E+07	2.21E+07	2.14E+07	7.87E+07	8.27E+07
193	441.373	Yellow; Blue; Violet; Green; Red	1.06E+07	6222177.706	1.72E+07	5.83E+07	5.02E+07
194	441.3733	Yellow; Blue; Violet; Green; Red	2067496.983	3.11E+07	1.78E+07	3.00E+07	1.14E+07
195	441.3939	Yellow; Blue; Violet; Green; Red	2.20E+07	2.74E+07	2.63E+07	3.47E+07	6.11E+07
196	441.3939	Yellow; Blue; Violet; Green; Red	1.70E+08	2.31E+08	2.12E+08	3.29E+08	4.77E+08
197	442.4256	Yellow; Blue; Violet; Green; Red	2.53E+07	1.05E+07	3.60E+07	7756284.4	3090445.164
198	443.352	Yellow; Blue; Violet; Green; Red	1.62E+07	1.99E+07	4.04E+07	1.48E+07	1.30E+07
199	443.3522	Yellow; Blue; Violet; Green; Red	8922624.935	1.10E+07	1.37E+07	1.60E+07	5.00E+07
200	444.2018	Yellow; Blue; Violet; Green; Red	7823786.296	2.40E+07	6998224.551	1208628.985	2929999.188
201	444.2018	Yellow; Blue; Violet; Green; Red	7823786.296	3.25E+07	6846388.066	1170122.235	2832179.28
202	447.4197	Yellow; Blue; Violet; Green; Red	2.43E+07	4707150.149	8134068.35	2684588.907	2146229.745
203	449.1572	Yellow; Blue; Violet; Green; Red	6609367.15	3.38E+07	8769779.263	1578941.601	3691242.718
204	449.1573	Yellow; Blue; Violet; Green; Red	9483360.965	2.96E+07	9124925.364	1636219.22	3887670.089
205	449.1573	Yellow; Blue; Violet; Green; Red	8005013.816	2.14E+07	8729607.509	1388721.936	2945754.641
206	449.3047	Yellow; Blue; Violet; Green; Red	1052677.92	1034077.898	1410999.542	1.95E+07	1209333.316
207	451.3207	Yellow; Blue; Violet; Green; Red	1.21E+07	4890308.787	6305752.06	3309863.335	3.79E+07

208	451.3571	Yellow; Blue; Violet; Green; Red	345780.2846	8005809.922	2129359.935	4.92E+07	1.00E+08
209	451.3571	Yellow; Blue; Violet; Green; Red	107135.3656	2278126.524	1528581.068	2.68E+07	2.23E+07
210	451.3571	Yellow; Blue; Violet; Green; Red	303597.0004	3358704.877	1.05E+07	3.46E+07	4.53E+07
211	453.319	Yellow; Blue; Violet; Green; Red	2.52E+07	1.27E+07	7100235.464	1.90E+07	4.73E+07
212	453.3341	Yellow; Blue; Violet; Green; Red	2.55E+08	7.26E+07	1.36E+08	3.12E+07	1.81E+07
213	453.3364	Yellow; Blue; Violet; Green; Red	4.83E+07	2.79E+07	4.79E+07	1.51E+07	2.28E+07
214	453.3364	Yellow; Blue; Violet; Green; Red	2.34E+07	3.00E+07	4.70E+07	1.92E+07	3.36E+07
215	453.3365	Yellow; Blue; Violet; Green; Red	2.98E+07	2.53E+07	4.20E+07	2.18E+07	1.99E+07
216	453.3365	Yellow; Blue; Violet; Green; Red	3.79E+07	3.44E+07	2.31E+07	4.53E+07	5.96E+07
217	453.3551	Yellow; Blue; Violet; Green; Red	8.97E+07	1.03E+08	6.38E+07	1.72E+08	1.98E+08
218	453.3726	Yellow; Blue; Violet; Green; Red	189247.3941	3195016.524	1.11E+07	5.93E+07	6.36E+07
219	455.3345	Yellow; Blue; Violet; Green; Red	2.16E+07	9541750.544	2.12E+07	1.89E+07	1.53E+07
220	455.3519	Yellow; Blue; Violet; Green; Red	3.80E+07	6467841.126	2.18E+07	6704791.728	5313189.821
221	455.3519	Yellow; Blue; Violet; Green; Red	3481799.163	80822.91006	1.84E+07	161931.186	84489.8105
222	455.352	Yellow; Blue; Violet; Green; Red	3.83E+07	3.83E+07	7.61E+07	1.16E+08	1.35E+08
223	455.352	Yellow; Blue; Violet; Green; Red	6.01E+07	1.56E+07	1.61E+07	2.36E+07	2.21E+07
224	455.352	Yellow; Blue; Violet; Green; Red	8.45E+07	3.17E+07	6.26E+07	2.07E+07	3.84E+07
225	455.352	Yellow; Blue; Violet; Green; Red	4.31E+07	3.66E+07	7.96E+07	5.76E+07	7.61E+07
226	455.3521	Yellow; Blue; Violet; Green; Red	6.71E+07	9356309.977	8239803.952	1635397.456	2063418.105

227	455.3521	Yellow; Blue; Violet; Green; Red	5.83E+07	1.12E+08	1.18E+08	1.05E+08	8.12E+07
228	455.3521	Yellow; Blue; Violet; Green; Red	1.38E+07	4.50E+07	2.21E+07	1.08E+08	4.38E+07
229	455.3521	Yellow; Blue; Violet; Green; Red	1.28E+08	6.43E+07	1.74E+08	6.23E+07	3.66E+07
230	455.3521	Yellow; Blue; Violet; Green; Red	5.40E+07	8172884.215	2.47E+07	7878386.275	4776072.65
231	455.3521	Yellow; Blue; Violet; Green; Red	7.01E+07	7.97E+07	1.35E+08	8.80E+07	5.46E+07
232	455.3521	Yellow; Blue; Violet; Green; Red	8.13E+07	8.80E+07	1.51E+08	1.32E+08	1.37E+08
233	455.3521	Yellow; Blue; Violet; Green; Red	5.91E+07	5.30E+07	9.98E+07	3.97E+07	2.29E+07
234	455.3521	Yellow; Blue; Violet; Green; Red	3.38E+07	2.47E+07	3.28E+07	1.25E+08	9.55E+07
235	455.3522	Yellow; Blue; Violet; Green; Red	4.85E+07	1.86E+07	2.40E+07	2.61E+07	2.42E+07
236	455.3732	Yellow; Blue; Violet; Green; Red	5.30E+07	7.62E+07	5.53E+07	1.15E+08	1.72E+08
237	456.4413	Yellow; Blue; Violet; Green; Red	396124.3658	1.92E+07	3375911.231	1154152.475	55273.52871
238	457.2582	Yellow; Blue; Violet; Green; Red	525971.6383	1.60E+07	4547642.177	945785.2085	932807.2349
239	457.3322	Yellow; Blue; Violet; Green; Red	2312988.663	2.73E+07	7585077.287	1.13E+07	7108829.954
240	457.3676	Yellow; Blue; Violet; Green; Red	1.64E+07	4.59E+07	6.90E+07	8.53E+07	8.40E+07
241	457.3677	Yellow; Blue; Violet; Green; Red	1.12E+07	1.09E+08	1.60E+08	2.21E+08	1.80E+08
242	457.3677	Yellow; Blue; Violet; Green; Red	1.41E+08	5.57E+07	1.22E+08	2.80E+07	2.85E+07
243	457.3678	Yellow; Blue; Violet; Green; Red	1.66E+07	4.12E+07	6.93E+07	7.99E+07	3.23E+08
244	457.3679	Yellow; Blue; Violet; Green; Red	2390412.137	5052381.992	8465481.311	4.47E+07	9.21E+07
245	459.3106	Yellow; Blue; Violet; Green; Red	3.14E+07	1.48E+07	2.67E+07	3.50E+07	1.93E+07

246	461.3837	Yellow; Blue; Violet; Green; Red	1.14E+07	1.24E+07	2.04E+07	3.34E+07	1.24E+07
247	463.2116	Yellow; Blue; Violet; Green; Red	166174.5114	6556401.477	903796.4677	384436.1361	12350.87622
248	463.2117	Yellow; Blue; Violet; Green; Red	786753.9292	8.68E+07	1.10E+07	2716853.437	134745.44
249	465.227	Yellow; Blue; Violet; Green; Red	28772.9971	1.30E+07	2353988.982	28838.29857	75473.80103
250	465.2996	Yellow; Blue; Violet; Green; Red	171561.67	499106.2086	239724.3218	4.87E+07	2252999.592
251	465.3729	Yellow; Blue; Violet; Green; Red	1265571.727	5.28E+07	2.09E+07	6.71E+07	1.62E+07
252	465.373	Yellow; Blue; Violet; Green; Red	1.58E+07	5.76E+08	1.15E+09	6.47E+08	8.05E+07
253	467.3153	Yellow; Blue; Violet; Green; Red	4463954.833	4380157.988	6198891.885	4.71E+07	8206156.196
254	467.3344	Yellow; Blue; Violet; Green; Red	1.22E+08	1.20E+08	8.31E+07	1.59E+08	2.22E+08
255	469.3312	Yellow; Blue; Violet; Green; Red	2858419.314	1.06E+07	3876277.163	1.77E+07	1.40E+07
256	469.3312	Yellow; Blue; Violet; Green; Red	4497759.866	1.86E+07	7318960.119	1.74E+07	2.91E+07
257	469.3313	Yellow; Blue; Violet; Green; Red	1.37E+07	9886373.432	3.62E+07	1.44E+07	2.57E+07
258	469.3315	Yellow; Blue; Violet; Green; Red	2707349.597	4928962.358	6.76E+08	8320797.457	8956782.008
259	469.3676	Yellow; Blue; Violet; Green; Red	497591.8336	3702676.536	1.06E+07	3.49E+07	4.34E+07
260	469.3677	Yellow; Blue; Violet; Green; Red	594477.3298	1.07E+07	5602505.712	5.17E+07	7.14E+07
261	469.3677	Yellow; Blue; Violet; Green; Red	178285.8422	1.93E+07	8798365.903	1.52E+08	6.93E+07
262	471.3315	Yellow; Blue; Violet; Green; Red	6035271.612	1.62E+07	1.54E+07	2.49E+07	5.71E+07
263	471.347	Yellow; Blue; Violet; Green; Red	3.23E+08	1.77E+08	3.08E+08	9.71E+07	2.49E+08
264	471.347	Yellow; Blue; Violet; Green; Red	3.67E+07	2.92E+07	4.76E+07	2.10E+07	2.18E+07

265	471.3471	Yellow; Blue; Violet; Green; Red	1.05E+08	2.19E+07	8367465.927	1.45E+07	1.75E+07
266	471.3471	Yellow; Blue; Violet; Green; Red	3.21E+07	3.07E+07	5.70E+07	2.02E+07	2.42E+07
267	471.3679	Yellow; Blue; Violet; Green; Red	6514625.434	1.69E+07	2.14E+07	4.82E+07	9.11E+07
268	471.3833	Yellow; Blue; Violet; Green; Red	176906.6471	3341081.27	7357474.898	4.11E+07	4.25E+07
269	472.3635	Yellow; Blue; Violet; Green; Red	9325378.36	2743749.578	1.20E+07	1359788.805	68341.68039
270	473.3627	Yellow; Blue; Violet; Green; Red	3.28E+07	2.10E+07	2.81E+07	1.29E+07	2.14E+07
271	475.3418	Yellow; Blue; Violet; Green; Red	748733.6134	2.81E+07	1252514.168	1836239.151	1289641.297
272	475.4512	Yellow; Blue; Violet; Green; Red	6.28E+07	1.74E+07	2.14E+07	8898016.845	2998860.715
273	477.3343	Yellow; Blue; Violet; Green; Red	1.04E+07	2.02E+07	6485222.542	8.09E+07	3.26E+07
274	481.222	Yellow; Blue; Violet; Green; Red	75376.14661	3.81E+07	3620635.266	310192.6484	431149.2716
275	481.2926	Yellow; Blue; Violet; Green; Red	2.30E+08	1.44E+08	2.49E+08	2.99E+08	1.30E+08
276	481.2926	Yellow; Blue; Violet; Green; Red	1.41E+08	6.28E+07	1.08E+08	1.09E+08	4.83E+07
277	481.2944	Yellow; Blue; Violet; Green; Red	374402.3517	497675.6833	607125.0041	1.19E+07	3081832.083
278	481.3313	Yellow; Blue; Violet; Green; Red	174400.4864	7.35E+07	6.35E+07	1.22E+08	3.47E+07
279	481.3499	Yellow; Blue; Violet; Green; Red	1.87E+07	9787412.349	1.41E+07	1.69E+07	3.50E+07
280	481.368	Yellow; Blue; Violet; Green; Red	3846312.222	5.37E+07	8.40E+07	6.81E+07	1.98E+07
281	481.3864	Yellow; Blue; Violet; Green; Red	2.78E+07	4.95E+07	2.95E+07	1.11E+08	1.53E+08
282	482.4569	Yellow; Blue; Violet; Green; Red	404780.8908	2.59E+07	2718640.397	4084.30902	3076.212052
283	482.457	Yellow; Blue; Violet; Green; Red	1678542.761	8.70E+07	8788974.644	21326.6	7613.158003

284	483.3101	Yellow; Blue; Violet; Green; Red	282531.6302	605942.2457	273272.1975	1.60E+08	4516190.371
285	483.3656	Yellow; Blue; Violet; Green; Red	1.24E+07	1.11E+07	1.11E+07	2.68E+07	9236134.433
286	483.3832	Yellow; Blue; Violet; Green; Red	1854154.297	8.98E+07	2.67E+07	1.04E+08	2.52E+07
287	483.3834	Yellow; Blue; Violet; Green; Red	3.44E+07	9.67E+08	1.92E+09	1.08E+09	1.47E+08
288	484.4726	Yellow; Blue; Violet; Green; Red	2315071.162	1.43E+08	5.89E+07	4.14E+07	6076209.28
289	485.1936	Yellow; Blue; Violet; Green; Red	182722.1674	1.87E+07	3549195.805	643070.0624	4510.847878
290	485.3261	Yellow; Blue; Violet; Green; Red	1411274.646	1053654.992	2548893.012	2.48E+07	4599178.895
291	485.3262	Yellow; Blue; Violet; Green; Red	3.91E+07	9513883	9609700.685	7896163.298	8270894.205
292	485.3472	Yellow; Blue; Violet; Green; Red	9037318.9	4.11E+07	4.99E+07	1.04E+08	1.81E+08
293	487.3052	Yellow; Blue; Violet; Green; Red	88296.7381	84578.67872	116235.2661	84408.57159	4.75E+07
294	487.3053	Yellow; Blue; Violet; Green; Red	133908.7518	148538.596	182859.173	249186.8887	3.50E+07
295	487.3416	Yellow; Blue; Violet; Green; Red	1049945.955	1245600.861	3.90E+08	1883435.317	3986020.476
296	487.3419	Yellow; Blue; Violet; Green; Red	3.31E+07	3.86E+07	6.21E+07	1.99E+07	1.86E+07
297	487.3421	Yellow; Blue; Violet; Green; Red	3925501.618	4441559.904	1.75E+07	4369014.981	5576995.853
298	488.3739	Yellow; Blue; Violet; Green; Red	28895.53322	75024.11845	2.20E+07	165222.4891	132894.5658
299	493.2809	Yellow; Blue; Violet; Green; Red	4.31E+07	2.00E+07	2.92E+07	2.56E+07	1.51E+07
300	493.3294	Yellow; Blue; Violet; Green; Red	2798631.306	6438022.606	6784916.514	1242691.412	1508520.677
301	493.3295	Yellow; Blue; Violet; Green; Red	448944.7644	402208.1511	2.57E+07	596504.7992	940531.3354
302	493.4615	Yellow; Blue; Violet; Green; Red	4.54E+07	1.22E+07	1.91E+07	6800889.146	2012859.542

303	495.3657	Yellow; Blue; Violet; Green; Red	3.31E+07	5.19E+07	3.26E+07	9.15E+07	1.22E+08
304	497.3245	Yellow; Blue; Violet; Green; Red	356188.923	5.44E+07	2744178.862	9482760.563	3151851.868
305	497.3624	Yellow; Blue; Violet; Green; Red	410826.6728	1.52E+07	1.07E+07	1.59E+08	7.09E+07
306	497.3627	Yellow; Blue; Violet; Green; Red	914595.5333	1.68E+07	2.24E+07	6.11E+07	2.38E+07
307	497.3627	Yellow; Blue; Violet; Green; Red	2258516.24	3.38E+07	3.91E+07	7.65E+07	1.71E+07
308	498.3791	Yellow; Blue; Violet; Green; Red	8261672.488	3.34E+07	1.41E+08	9.47E+07	2.10E+07
309	499.3785	Yellow; Blue; Violet; Green; Red	6.23E+07	1.50E+09	2.21E+09	1.61E+09	3.47E+08
310	499.436	Yellow; Blue; Violet; Green; Red	4.08E+07	1.46E+07	3131669.727	2665747.359	4785220.547
311	500.3369	Yellow; Blue; Violet; Red	0	63776.48009	1448.398553	1.93E+07	464405.589
312	500.4675	Yellow; Blue; Violet; Green; Red	591024.0445	1.36E+07	2236766.597	68060.14514	129701.5428
313	500.4675	Yellow; Blue; Violet; Green; Red	840556.3414	3.78E+07	5010446.281	41437.22536	117286.3064
314	500.4676	Yellow; Blue; Violet; Green; Red	145728.8116	1.63E+07	7.66E+07	6.94E+07	9097497.313
315	501.3786	Yellow; Blue; Violet; Green; Red	3.08E+07	3.03E+07	3.83E+07	5.15E+07	7.40E+07
316	503.2042	Yellow; Blue; Violet; Green; Red	11167.25545	6857317.739	653058.6717	25200.30032	237544.3638
317	504.3684	Yellow; Blue; Violet; Green; Red	1279723.848	1253275.116	4.79E+08	1825581.346	1573050.469
318	505.2926	Yellow; Blue; Violet; Green; Red	29912.7322	161870.8389	34567.8216	1.17E+07	638553.8845
319	505.3523	Yellow; Blue; Violet; Green; Red	1.03E+07	1.54E+07	1.26E+07	3.55E+07	7.80E+07
320	506.4547	Yellow; Blue; Violet; Green; Red	241547.1977	3.05E+07	1.15E+07	1.57E+07	1406856.123
321	507.2278	Yellow; Blue; Violet; Green; Red	2126296.431	8667466.086	4530029.314	3269956.396	1512713.812

322	508.4728	Yellow; Blue; Violet; Green; Red	7.20E+07	3.94E+07	6.53E+07	3.34E+07	1.78E+07
323	509.2877	Yellow; Blue; Violet; Green; Red	67136.8603	53961.90028	88823.82566	64650.45907	8.39E+07
324	509.324	Yellow; Blue; Violet; Green; Red	2385397.565	2191750.3	3.37E+08	2690985.495	2695816.035
325	509.3242	Yellow; Blue; Violet; Green; Red	3841376.547	2320510.939	4.90E+07	1669659.501	1870189.885
326	510.4015	Yellow; Blue; Violet; Green; Red	2.27E+07	1795636.794	2645784.594	670571.2949	69129.55849
327	511.3402	Yellow; Blue; Violet; Green; Red	681416.0885	1.93E+07	819167.0039	4104614.777	1275738.74
328	511.3606	Yellow; Blue; Violet; Green; Red	5111688.933	1.46E+07	1.18E+07	3.54E+07	6.11E+07
329	512.5039	Yellow; Blue; Violet; Green; Red	7.16E+07	4.89E+07	7.23E+07	2.27E+07	1.74E+07
330	512.5039	Yellow; Blue; Violet; Green; Red	6.76E+07	2.68E+07	5.12E+07	2.27E+07	1.73E+07
331	513.4516	Yellow; Blue; Violet; Green; Red	1.55E+07	5.61E+07	6.25E+07	8.93E+07	7.83E+07
332	514.4468	Yellow; Blue; Violet; Green; Red	123879.6155	9852930.361	1116810.16	14035.04725	12132.10689
333	515.3001	Yellow; Blue; Violet; Green; Red	260495.5791	216447.5251	229281.5652	9317018.039	1253092.667
334	516.3325	Yellow; Blue; Violet; Green; Red	3481.044202	78808.87255	4601.408125	1.63E+07	1407176.594
335	520.3399	Yellow; Blue; Violet; Green; Red	1.54E+07	1.98E+07	1.23E+08	4.43E+07	5459693.807
336	520.3607	Yellow; Blue; Violet; Green; Red	4138914.681	1.62E+07	3.19E+07	2.76E+07	1.03E+07
337	521.2876	Yellow; Blue; Violet; Green; Red	143498.9618	513129.5231	168191.2466	1.73E+07	4988714.548
338	521.3603	Yellow; Blue; Violet; Green; Red	3619097.669	9.84E+07	1.15E+08	1.09E+08	3.24E+07
339	522.3557	Yellow; Blue; Violet; Green; Red	5.18E+07	3.20E+07	1.05E+08	1.49E+07	1404368.994
340	522.4495	Yellow; Violet; Green; Red	535739.1016	1.85E+07	2150062.702	11649.72688	0

341	523.3761	Yellow; Blue; Violet; Green; Red	545097.1738	5.31E+07	1.05E+08	6.77E+07	7195038.421
342	524.3951	Yellow; Blue; Violet; Green; Red	820197.785	8710788.984	3.07E+07	7.68E+07	3.10E+07
343	524.4171	Yellow; Blue; Violet; Green; Red	2.07E+07	1.84E+07	3.37E+07	6290104.904	1492448.477
344	525.2979	Yellow; Blue; Violet; Red	0	17237.98014	2.76E+07	19823.88165	11649.45824
345	525.3193	Yellow; Blue; Violet; Green; Red	533002.1297	1.05E+07	1390184.046	2459191.432	890036.2519
346	525.3399	Yellow; Blue; Violet; Green; Red	6568088.194	1.37E+07	1.49E+07	3.45E+07	2.85E+07
347	525.34	Yellow; Blue; Violet; Green; Red	1.08E+07	1.99E+07	2.79E+07	6.64E+07	1.12E+08
348	526.2226	Yellow; Blue; Violet; Green; Red	1306.924257	977748.3708	1324282.314	1.56E+07	6395367.838
349	527.4674	Yellow; Blue; Violet; Green; Red	1.34E+08	1.08E+08	8.52E+07	7.95E+07	1.19E+08
350	529.2097	Yellow; Blue; Violet; Green; Red	2465209.629	8670023.557	5308387.962	4209303.811	1953348.985
351	529.3502	Yellow; Blue; Violet; Green; Red	827856.5995	9670205.875	3.19E+07	9.69E+07	3.77E+07
352	532.3273	Yellow; Blue; Violet; Green; Red	26736.09357	25823.82511	10887.72708	1.38E+07	3702526.374
353	533.3839	Yellow; Blue; Violet; Green; Red	2.20E+07	5.92E+07	3.99E+07	1.48E+08	2.53E+08
354	533.4543	Yellow; Blue; Violet; Green; Red	5.64E+07	1.88E+07	2.05E+07	1.08E+07	3726439.631
355	534.4882	Yellow; Blue; Violet; Green; Red	3.22E+07	3.39E+07	5.09E+07	2.79E+07	2.40E+07
356	534.4884	Yellow; Blue; Violet; Green; Red	2.93E+07	5.24E+07	6.04E+07	3.63E+07	3.81E+07
357	535.2706	Yellow; Violet; Green; Red	464127.5844	672261.4524	1.42E+07	1248.029013	0
358	535.4335	Yellow; Blue; Violet; Green; Red	2.06E+07	4.31E+07	3.57E+07	7.56E+07	5.78E+07
359	536.1656	Yellow; Blue; Violet; Green; Red	7932917.594	8430054.55	3.21E+07	3.80E+07	5.51E+07

360	536.429	Yellow; Blue; Violet; Green; Red	179891.0429	1.26E+07	999385.2737	4257.352161	7630.334421
361	537.2827	Yellow; Blue; Violet; Green; Red	106801.8819	129646.3535	97033.03355	1.02E+07	4092483.834
362	538.4328	Yellow; Blue; Violet; Green; Red	3.23E+07	2.40E+07	1.70E+07	2371826.085	84663.22367
363	541.3712	Yellow; Blue; Violet; Green; Red	6.08E+07	5.78E+07	4.42E+07	8.12E+07	1.11E+08
364	541.4465	Yellow; Blue; Violet; Green; Red	3.68E+07	4.09E+07	4.58E+07	7.83E+07	8.08E+07
365	542.4781	Yellow; Blue; Violet; Green; Red	7244130.381	6.78E+08	6.47E+07	507327.6703	341784.9324
366	542.4782	Yellow; Blue; Violet; Green; Red	3.20E+07	2.40E+09	2.42E+08	1677865.756	931770.9944
367	544.4728	Yellow; Blue; Violet; Green; Red	4.39E+07	3.74E+07	1.95E+07	8755916.528	5542751.732
368	545.2899	Yellow; Blue; Violet; Green; Red	10300.33995	17386.8882	2717476.245	4.09E+07	5331861.848
369	546.4883	Yellow; Blue; Violet; Green; Red	3.30E+08	3.09E+08	9.74E+07	8.61E+07	5.98E+07
370	547.3265	Yellow; Violet; Green; Red	28466.52444	1916321.805	2.86E+07	58220.53111	0
371	548.5039	Yellow; Blue; Violet; Green; Red	1.87E+07	5.05E+07	5.79E+07	6.34E+07	3.35E+07
372	549.4128	Yellow; Blue; Violet; Green; Red	1.74E+07	2.40E+07	1.83E+07	6.14E+07	6.46E+07
373	549.4492	Yellow; Blue; Violet; Green; Red	6.30E+07	5.10E+07	3.20E+07	4.12E+07	6.41E+07
374	551.2984	Yellow; Blue; Violet; Green; Red	12701.5626	21204.90703	23061.90081	9337016.697	331524.7234
375	561.4149	Yellow; Blue; Violet; Green; Red	5201493.362	1.38E+07	1.12E+07	3.24E+07	8.12E+07
376	563.1703	Yellow; Blue; Violet; Green; Red	1.09E+07	2.38E+08	1.92E+08	4.25E+08	3.95E+08
377	563.1704	Yellow; Blue; Violet; Green; Red	243434.9481	3768541.414	5829212.905	2.31E+07	2.09E+07
378	563.4283	Yellow; Blue; Violet; Green; Red	3.71E+07	3.77E+07	3.88E+07	7.66E+07	7.36E+07

379	564.46	Yellow; Blue; Violet; Green; Red	2.82E+07	1.20E+09	1.54E+08	2320600.527	992341.2171
380	564.4602	Yellow; Blue; Violet; Green; Red	6082042.566	4.23E+08	3.95E+07	755904.7323	311703.9873
381	567.4229	Yellow; Blue; Violet; Green; Red	1.66E+08	1.04E+08	8.72E+07	1.03E+07	407947.7439
382	571.2693	Yellow; Blue; Violet; Green; Red	3149.27616	40885.31289	4490898.325	7.02E+07	7428109.856
383	572.4682	Yellow; Blue; Violet; Green; Red	28391.68829	21318.31308	1.93E+07	2801539.617	6140.156376
384	572.5251	Yellow; Blue; Violet; Green; Red	8.90E+07	6.96E+07	6.79E+07	7.64E+07	5.56E+07
385	573.3419	Yellow; Blue; Violet; Green; Red	33204.89187	802593.3496	1.29E+07	49052.00556	20414.24265
386	576.3693	Yellow; Red	0	4246643.676	0	1547682.592	0
387	577.4233	Yellow; Blue; Violet; Green; Red	50442.22	72093.49196	3.53E+07	6369899.591	36524.58885
388	579.4983	Yellow; Blue; Violet; Green; Red	5.87E+07	2.33E+07	1.85E+07	1.24E+07	5026347.346
389	580.4335	Yellow; Blue; Violet; Green; Red	954498.706	2.73E+07	4946167.246	10661.45449	0
390	583.4936	Yellow; Blue; Violet; Green; Red	1.34E+07	1.96E+07	4.06E+07	1.83E+07	1.30E+07
391	587.4885	Yellow; Blue; Violet; Green; Red	5487114.54	1.81E+07	1.75E+07	1.04E+08	1.17E+08
392	588.4113	Yellow; Blue; Violet; Green; Red	8.01E+07	8287287.061	8328094.64	5458925.257	1.01E+07
393	589.2797	Yellow; Blue; Violet; Green; Red	3511.753742	25922.41356	2949596.619	4.48E+07	1401109.974
394	589.4047	Yellow; Blue; Violet; Green; Red	6.81E+07	4.72E+07	2.95E+07	6502912.982	305312.3602
395	589.41	Yellow; Blue; Violet; Green; Red	1.67E+07	2.43E+07	2.22E+07	1.08E+08	1.33E+08
396	591.4259	Yellow; Blue; Violet; Green; Red	1.02E+08	1.15E+08	1.45E+08	1.51E+08	9.36E+07
397	593.276	Yellow; Blue; Violet; Green; Red	7.85E+07	3.66E+07	5.70E+07	1.08E+07	1.36E+07

398	593.3657	Yellow; Blue; Violet; Green; Red	6.55E+07	6260545.331	6312546.383	4266180.937	9530359.809
399	594.3795	Yellow; Blue; Violet; Red	0	3.47E+07	1134.62976	7443640.051	19668.76352
400	595.4544	Yellow; Blue; Violet; Green; Red	1.93E+08	1.15E+08	6.68E+07	8230477.24	520869.6556
401	599.4097	Yellow; Blue; Violet; Green; Red	24295.93566	9698837.372	138393.1262	5565973.839	1.81E+08
402	599.4098	Yellow; Blue; Violet; Green; Red	17359.47936	5468248.069	82690.76096	5552088.106	9.96E+07
403	599.4103	Yellow; Blue; Violet; Green; Red	14204.46814	8899036.407	53680.86051	5986197.235	2.80E+08
404	600.4125	Yellow; Blue; Violet; Green; Red	348266.2076	8640167.303	5.34E+07	8666622.453	1851422.256
405	601.3712	Yellow; Blue; Violet; Green; Red	1.13E+07	1.92E+07	1.56E+07	4.59E+07	6.29E+07
406	601.4677	Yellow; Blue; Violet; Green; Red	9403476.537	4.11E+07	4.55E+07	1.47E+08	1.25E+08
407	601.5044	Yellow; Blue; Violet; Green; Red	9734932.994	1.02E+07	2.30E+07	1.45E+07	7994798.326
408	605.4392	Yellow; Blue; Violet; Green; Red	2.09E+07	4842437.246	1.79E+07	1.41E+07	1403878.975
409	607.2917	Yellow; Blue; Violet; Green; Red	5.98E+07	2.27E+07	7.15E+07	3135881.061	7836726.507
410	607.4208	Yellow; Blue; Violet; Green; Red	1.79E+07	2.43E+07	2.92E+07	8.43E+07	1.13E+08
411	609.271	Yellow; Blue; Violet; Green; Red	1.77E+07	8683783.092	1.66E+07	3653200.957	2910174.329
412	609.271	Yellow; Blue; Violet; Green; Red	7.58E+07	3.00E+07	3.47E+07	1.33E+07	8964610.121
413	609.4704	Yellow; Blue; Violet; Green; Red	5618927.568	1.78E+07	1.34E+07	8.61E+07	6.99E+07
414	609.4705	Yellow; Blue; Violet; Green; Red	5618927.568	1.76E+07	1.22E+07	9.41E+07	1.21E+08
415	609.4879	Yellow; Blue; Violet; Green; Red	1.09E+08	4.17E+07	9.76E+07	1.90E+07	6857822.431
416	609.488	Yellow; Blue; Violet; Green; Red	1.62E+08	5.84E+07	1.16E+08	1.45E+07	6857822.431

417	611.4521	Yellow; Blue; Violet; Green; Red	5.03E+07	2.86E+07	5.08E+07	5.13E+07	4.71E+07
418	613.3892	Yellow; Blue; Violet; Green; Red	31644.68128	1.43E+07	204801.8303	1.02E+07	2.11E+08
419	616.3611	Yellow; Red	0	1.89E+07	0	5142074.263	0
420	616.4077	Yellow; Blue; Violet; Green; Red	55416.60545	1.15E+07	1645900.3	3440224.557	3795313.439
421	617.3841	Yellow; Blue; Violet; Green; Red	279406.6636	8687594.911	4604654.559	6.20E+07	5.86E+07
422	617.4361	Yellow; Blue; Violet; Green; Red	7.45E+07	5.52E+07	2.74E+07	1.05E+07	432104.8491
423	619.4912	Yellow; Blue; Violet; Green; Red	8.72E+07	3.20E+07	2.61E+07	2.01E+07	8708467.275
424	620.3773	Yellow; Blue; Violet; Green; Red	8575496.524	1.49E+07	3.03E+07	1.84E+07	1.03E+07
425	622.3746	Yellow; Red	0	8355318.128	0	1796252.467	0
426	622.3944	Yellow; Blue; Violet; Green; Red	179183.4224	5379798.528	1.68E+07	5506094.738	858231.3346
427	623.4496	Yellow; Blue; Violet; Green; Red	1.08E+07	3.74E+07	4.18E+07	1.49E+08	1.19E+08
428	623.4862	Yellow; Blue; Violet; Green; Red	1.93E+07	3.41E+07	5.88E+07	3.43E+07	1.72E+07
429	625.2659	Yellow; Blue; Violet; Green; Red	2.56E+07	1.18E+07	1.22E+07	6746264.806	5362685.799
430	629.3835	Yellow; Blue; Violet; Green; Red	20802.52714	4860109.336	123252.0751	2833231.237	6.67E+07
431	629.4027	Yellow; Blue; Violet; Green; Red	1.81E+07	5.50E+07	2.93E+07	1.94E+08	2.14E+08
432	635.371	Yellow; Blue; Violet; Green; Red	16649.0088	1.26E+07	109226.0932	1.27E+07	1.77E+08
433	637.4654	Yellow; Blue; Violet; Green; Red	2.31E+07	1.77E+07	2.89E+07	3.83E+07	5.42E+07
434	638.3896	Yellow; Blue; Violet; Green; Red	30334.39693	8101816.788	2333288.92	1362208.498	2217880.23
435	643.2575	Yellow; Blue; Violet; Green; Red	1.45E+07	2.42E+07	3.53E+07	2.45E+07	1.10E+07
436	644.3563	Yellow; Red	0	4275619.77	0	1294066.826	0

437	647.5096	Yellow; Blue; Violet; Green; Red	7903797.979	1.70E+07	2.18E+07	6.66E+07	5.18E+07
438	647.5097	Yellow; Blue; Violet; Green; Red	1.04E+07	6.11E+07	8.15E+07	2.08E+08	2.24E+08
439	647.5097	Yellow; Blue; Violet; Green; Red	1.28E+07	3.11E+07	2.94E+07	5.82E+07	2.17E+08
440	649.4807	Yellow; Blue; Violet; Green; Red	4.90E+07	2.35E+07	2.87E+07	9522025.963	3099588.017
441	651.4446	Yellow; Blue; Violet; Green; Red	7.33E+07	4.63E+07	7.23E+07	9.14E+07	7.87E+07
442	651.4808	Yellow; Blue; Violet; Green; Red	5250459.603	1.43E+07	1.45E+07	1.45E+07	4.90E+07
443	651.4809	Yellow; Blue; Violet; Green; Red	7395564.446	1.75E+07	2.02E+07	3.99E+07	1.23E+08
444	651.5059	Yellow; Blue; Violet; Green; Red	1.35E+08	6.30E+07	7.70E+07	1.86E+07	1.88E+07
445	652.4036	Yellow; Blue; Violet; Green; Red	2.27E+07	5.92E+07	1.86E+08	9.31E+07	1.32E+07
446	656.3504	Yellow; Violet; Green	2.23E+07	654.8244641	14534.39264	0	0
447	657.434	Yellow; Blue; Violet; Green; Red	5428611.247	1.59E+07	1.23E+07	6.13E+07	9.40E+07
448	661.4889	Yellow; Blue; Violet; Green; Red	5535829.973	1.10E+07	1.13E+07	1.82E+07	3.84E+07
449	661.4891	Yellow; Blue; Violet; Green; Red	1969360.959	6011680.586	8722728.016	1.33E+07	2.16E+07
450	663.389	Yellow; Blue; Violet; Green; Red	38038.02205	9014177.779	3201530.096	3.09E+07	1.46E+07
451	663.4543	Yellow; Blue; Violet; Green; Red	3.60E+07	4.49E+07	5.07E+07	6.57E+07	6.16E+07
452	665.5216	Yellow; Blue; Violet; Green; Red	1.32E+08	7.23E+07	4.67E+07	2.68E+07	1.62E+07
453	669.4913	Yellow; Blue; Violet; Green; Red	1.12E+07	5.65E+07	6.86E+07	1.89E+08	1.84E+08
454	669.4914	Yellow; Blue; Violet; Green; Red	1.58E+07	4.87E+07	4.71E+07	1.46E+08	3.44E+08
455	671.5827	Yellow; Blue; Violet; Green; Red	1.32E+07	2.73E+07	3.42E+07	8.12E+07	1.05E+08

456	672.4949	Yellow; Blue; Violet; Green; Red	1.73E+07	1863836.51	189965.1129	555815.5124	5007568.686
457	1345.806	Yellow	0	1.30E+07	0	0	0
458	673.4876	Yellow; Blue; Violet; Green; Red	7.56E+07	3.79E+07	3.70E+07	1.46E+07	1.30E+07
459	677.5005	Yellow; Blue; Violet; Green; Red	9.93E+07	1.53E+08	1.74E+08	1.48E+08	1.30E+08
460	677.5697	Yellow; Blue; Violet; Green; Red	5746171.664	2.32E+07	3.67E+07	8.69E+07	4.57E+07
461	679.5372	Yellow; Blue; Violet; Green; Red	1.39E+08	6.46E+07	6.85E+07	6.42E+07	6.64E+07
462	681.2123	Yellow; Blue; Violet; Green; Red	3894522.723	9.64E+07	7.74E+07	1.82E+08	1.79E+08
463	683.4709	Yellow; Blue; Violet; Green; Red	9139284.482	1.56E+07	1.97E+07	1.93E+07	7.63E+07
464	685.4359	Yellow; Blue; Violet; Green; Red	3.69E+07	3.20E+07	3.91E+07	4.82E+07	3.01E+07
465	685.4891	Yellow; Blue; Violet; Green; Red	1.80E+07	1.93E+07	2.22E+07	1.89E+07	1.50E+07
466	687.5035	Yellow; Blue; Violet; Green; Red	6.29E+07	3.97E+07	2.76E+07	1.81E+07	2.19E+07
467	692.396	Yellow; Blue; Violet; Green; Red	1.31E+07	4.67E+07	1.19E+08	7.80E+07	1.68E+07
468	693.553	Yellow; Blue; Violet; Green; Red	1.50E+08	8.43E+07	9.69E+07	8.46E+07	7.82E+07
469	693.5643	Yellow; Blue; Violet; Green; Red	1.35E+07	2.71E+07	3.05E+07	9.75E+07	1.26E+08
470	693.5643	Yellow; Blue; Violet; Green; Red	4604851.959	1.53E+07	1.88E+07	2.68E+07	4.22E+07
471	696.5414	Yellow; Blue; Violet; Green; Red	9.80E+07	8.22E+07	1.22E+08	5.73E+07	5.02E+07
472	696.5415	Yellow; Blue; Violet; Green; Red	1.35E+08	1.50E+08	2.51E+08	1.90E+08	1.23E+08
473	697.465	Yellow; Blue; Violet; Green; Red	702851.8974	1.04E+07	122609.2977	396918.1214	542403.6059
474	697.4865	Yellow; Blue; Violet; Green; Red	4797078.516	1.52E+07	1.69E+07	5.62E+07	3.51E+07

475	698.2389	Yellow; Blue; Violet; Green; Red	2300036.725	5.74E+07	3.63E+07	2.61E+08	2.23E+08
476	699.2229	Yellow; Blue; Violet; Green; Red	3350254.659	5.19E+07	3.84E+07	9.59E+07	9.02E+07
477	701.5189	Yellow; Blue; Violet; Green; Red	6.26E+07	2.97E+07	2.24E+07	3.63E+07	3.33E+07
478	703.194	Yellow; Blue; Violet; Green; Red	966024.2247	2.15E+07	1.39E+07	6.77E+07	5.11E+07
479	707.5432	Yellow; Blue; Violet; Green; Red	4510367.309	1.30E+07	1.93E+07	2.72E+07	2.44E+07
480	708.5413	Yellow; Blue; Violet; Green; Red	8.69E+07	9.55E+07	1.79E+07	3.18E+07	3.37E+07
481	708.5423	Yellow; Blue; Violet; Green; Red	2.00E+07	2.32E+07	2.92E+07	4.20E+07	3.77E+07
482	709.5482	Yellow; Blue; Violet; Green; Red	0	2.10E+07	6386870.607	2.53E+07	1.18E+07
483	710.5572	Yellow; Blue; Violet; Green; Red	3.13E+07	1.20E+08	2.17E+08	2.99E+08	1.55E+08
484	714.552	Yellow; Blue; Violet; Green; Red	1.67E+08	1.94E+08	2.99E+08	2.23E+08	1.46E+08
485	714.5521	Yellow; Blue; Violet; Green; Red	1.10E+08	9.57E+07	1.37E+08	6.42E+07	4.66E+07
486	714.5522	Yellow; Blue; Violet; Green; Red	1.13E+08	1.17E+08	1.61E+08	8.67E+07	7.39E+07
487	715.5347	Yellow; Blue; Violet; Green; Red	7.33E+07	4.18E+07	3.42E+07	4.84E+07	5.41E+07
488	717.5141	Yellow; Blue; Violet; Green; Red	0	7878802.225	2159858.845	1.96E+07	7356879.483
489	717.5643	Yellow; Blue; Violet; Green; Red	1.93E+08	1.38E+08	1.30E+08	1.40E+08	1.24E+08
490	719.4465	Yellow; Blue; Violet; Green; Red	949202.8116	1.65E+07	180449.0761	578313.2987	934436.1682
491	720.2808	Yellow; Blue; Violet ;Red	0	9333748.607	407446.77	1.27E+07	1.06E+07
492	720.5263	Yellow; Blue; Violet; Green; Red	1.52E+07	1.71E+07	2.29E+07	1.71E+07	1.33E+07
493	723.5568	Yellow; Blue; Violet; Green; Red	6.00E+07	2.85E+07	4.71E+07	1.08E+07	4583831.594

494	723.6145	Yellow; Blue; Violet; Green; Red	6.14E+07	3.84E+07	3.68E+07	4.35E+07	5.38E+07
495	724.3393	Yellow; Blue; Violet; Green; Red	1.38E+07	2.35E+07	2.82E+07	2.42E+07	1.33E+07
496	724.5363	Yellow; Blue; Violet; Green; Red	3.21E+07	3.31E+07	2.42E+07	1.51E+07	1.44E+07
497	725.4815	Yellow; Blue; Violet; Green; Red	8.45E+07	5.26E+07	7.57E+07	9.72E+07	8.56E+07
498	728.5676	Yellow; Blue; Violet; Green; Red	4.88E+07	1.33E+08	2.16E+08	2.98E+08	1.86E+08
499	728.5677	Yellow; Blue; Violet; Green; Red	4.31E+07	1.23E+08	2.13E+08	3.03E+08	1.56E+08
500	729.2944	Yellow; Blue; Violet; Green; Red	2.53E+07	3.83E+07	5.74E+07	4.08E+07	2.12E+07
501	731.5303	Yellow; Blue; Violet; Red	0	2.22E+07	5070772.332	3.32E+07	1.61E+07
502	733.5584	Yellow; Blue; Violet; Green; Red	4956500.877	1.18E+07	4463095.209	1.96E+07	3.43E+07
503	733.5587	Yellow; Blue; Violet; Green; Red	1.34E+07	1.43E+07	9102544.611	2.22E+07	7.49E+07
504	733.5589	Yellow; Blue; Violet; Green; Red	1.05E+07	2.69E+07	1.70E+07	6.05E+07	1.55E+08
505	736.5337	Yellow; Blue; Violet; Green; Red	6.20E+07	9.43E+07	9.79E+07	1.09E+08	5.92E+07
506	736.5338	Yellow; Blue; Violet; Green; Red	4.34E+07	5.23E+07	4.63E+07	3.58E+07	2.16E+07
507	740.2496	Yellow; Blue; Violet; Green; Red	506243.8969	2.04E+07	1.34E+07	7.73E+07	6.10E+07
508	740.5311	Yellow; Blue; Violet; Green; Red	3.01E+07	4.23E+07	1.07E+07	1.50E+07	2.02E+07
509	741.6241	Yellow; Blue; Violet; Green; Red	2279903.009	4352237.578	1.45E+07	609467.1099	523214.5416
510	742.5834	Yellow; Blue; Violet; Green; Red	6013843.117	1.93E+07	4.01E+07	2.97E+07	3.31E+07
511	745.5956	Yellow; Blue; Violet; Green; Red	5.11E+08	4.24E+08	3.71E+08	3.63E+08	3.61E+08
512	746.5783	Yellow; Blue; Violet; Green; Red	9.74E+07	1.40E+08	1.49E+08	1.87E+08	1.41E+08

513	747.6112	Yellow; Blue; Violet; Green; Red	1.34E+08	1.69E+08	1.42E+08	1.69E+08	1.78E+08
514	750.5495	Yellow; Blue; Violet; Green; Red	3.62E+07	8.23E+07	1.05E+08	1.78E+08	8.96E+07
515	751.5334	Yellow; Blue; Violet; Green; Red	9.76E+07	1.60E+08	1.35E+08	2.25E+08	1.64E+08
516	755.3401	Yellow; Violet; Green; Red	1.77E+07	3320.260283	1829.995281	5627.580275	0
517	756.5259	Yellow; Blue; Violet; Green; Red	11475.21983	1044.797621	147448.4283	2.40E+07	1.06E+07
518	1520.6602	Yellow; Blue; Violet; Green; Red	9413778.353	1.36E+07	1.97E+07	1.20E+07	1.21E+07
519	762.573	Yellow; Blue; Violet; Green; Red	390277.6571	1562206.664	3747707.324	1.67E+07	3291662.247
520	763.5482	Yellow; Blue; Violet; Green; Red	4.02E+07	2.42E+07	3.72E+07	1.09E+07	3314799.473
521	763.606	Yellow; Blue; Violet; Green; Red	4048941.3	6443125.854	2.46E+07	1420075.289	1301541.524
522	768.281	Yellow; Blue; Violet; Green; Red	512844.9539	7.28E+07	9060979.014	1.74E+08	1.55E+08
523	769.2948	Green; Red	1389.890956	0	0	5144617.33	0
524	769.6554	Yellow; Blue; Violet; Green; Red	1525321.674	2632544.638	1.07E+07	92751.18868	147395.6158
525	773.2361	Yellow; Blue; Violet; Green; Red	145730.4494	1.73E+07	3019558.804	4.03E+07	4.18E+07
526	779.6015	Yellow; Blue; Violet; Green; Red	2.41E+07	2.57E+07	3.03E+07	3.11E+07	2.65E+07
527	779.6016	Yellow; Blue; Violet; Green; Red	1.14E+07	1.80E+07	2.39E+07	7.68E+07	7.28E+07
528	1562.6707	Yellow; Blue; Violet; Green; Red	3467826.24	1.20E+07	1.34E+07	9834402.902	4519873.886
529	782.6659	Yellow; Blue; Violet; Green; Red	2.16E+07	6713564.286	4.47E+07	4607663.784	65040.67052
530	784.534	Yellow; Blue; Violet; Green; Red	6.29E+07	5.79E+07	1.54E+07	2.67E+07	2.83E+07
531	789.21	Yellow; Blue; Violet; Green; Red	91622.20863	1.18E+07	2568997.677	2.68E+07	2.60E+07

532	791.6371	Yellow; Blue; Violet; Green; Red	3687301.036	6886159.393	2.33E+07	468063.8325	559663.6954
533	791.6373	Yellow; Blue; Violet; Green; Red	3020013.011	4496392.427	1.65E+07	708818.6845	273395.8799
534	793.5802	Yellow; Blue; Violet; Green; Red	5299574.316	1.05E+07	3114310.364	3.67E+07	2.15E+07
535	794.6066	Yellow; Blue; Violet; Green; Red	2515831.1	1.69E+07	1265007.092	2.36E+07	5886.011398
536	795.2631	Yellow; Blue; Violet; Green	115310.7778	6566745.56	13645.35106	0	51332.98326
537	799.5184	Yellow; Blue; Violet; Green; Red	2.21E+07	1.50E+07	1.83E+07	2.17E+07	1.23E+07
538	1601.7421	Yellow; Blue; Violet; Green; Red	1.45E+07	3.19E+07	6.20E+07	3.32E+07	2.97E+07
539	802.4017	Yellow; Blue; Violet; Green; Red	3.90E+07	3.79E+07	1.25E+08	1.07E+08	1.96E+07
540	1606.6973	Yellow; Blue; Violet; Green; Red	1.23E+07	2.79E+07	4.81E+07	2.73E+07	2.14E+07
541	806.5157	Yellow; Blue; Violet; Green; Red	6.60E+07	6.00E+07	2.02E+07	3.42E+07	3.65E+07
542	807.3569	Yellow; Blue; Violet; Green; Red	3.09E+07	2.40E+07	8.56E+07	7.48E+07	1.23E+07
543	810.3764	Yellow; Blue; Violet; Green; Red	2.65E+07	3.92E+07	5.04E+07	2.99E+07	1.46E+07
544	815.3314	Yellow; Blue; Violet; Green; Red	4.05E+07	5.39E+07	7.44E+07	3.92E+07	2.57E+07
545	816.2812	Yellow; Blue; Violet; Green; Red	2.03E+08	1.37E+09	1.28E+09	1.90E+09	1.79E+09
546	821.2362	Yellow; Blue; Violet; Green; Red	5.02E+07	2.99E+08	2.65E+08	3.78E+08	3.37E+08
547	1643.7526	Yellow; Blue; Violet; Green; Red	6608254.463	3.15E+07	4.57E+07	1.80E+07	8344002.93
548	823.5548	Yellow; Blue; Violet; Green; Red	399899.553	231734.7933	1.16E+07	3379030.983	1.11E+07
549	824.6767	Yellow; Blue; Violet; Green; Red	6958987.752	1847266.614	4.47E+07	1311410.027	1581.810422
550	1648.7077	Yellow; Blue; Violet; Green; Red	7407049.558	2.79E+07	3.67E+07	1.30E+07	7452829.018

551	825.4979	Yellow; Blue; Violet; Green; Red	1.05E+07	5976448.658	1.68E+07	3880621.809	75634.39233
552	1653.7271	Yellow; Blue; Violet; Green; Red	4515440.771	1.13E+07	1.88E+07	1.16E+07	9574745.584
553	830.2604	Yellow; Blue; Violet; Green; Red	1171547.875	1.81E+07	1.10E+07	6.82E+07	3.70E+07
554	831.3629	Yellow; Blue; Green	1347.55266	1524.803687	0	0	3.99E+07
555	832.2758	Yellow; Blue; Violet; Green; Red	4502.475947	3589448.575	1436152.654	1.19E+07	1.38E+07
556	832.276	Yellow; Blue; Violet; Green; Red	563539.1829	8079493.071	8488200.793	2.01E+07	1.36E+07
557	835.2156	Yellow; Blue; Violet; Green; Red	409943.2369	8353689.46	5718781.958	1.46E+07	1.30E+07
558	1670.753	Yellow; Blue; Violet; Green; Red	4815169.793	1.03E+07	1.87E+07	1.22E+07	9756738.108
559	837.2091	Yellow; Blue; Violet; Green; Red	2.38E+07	9.35E+07	7.98E+07	1.10E+08	1.01E+08
560	838.4864	Yellow; Blue; Violet; Green; Red	1833164.37	2.11E+07	4.92E+07	2.40E+07	1.02E+07
561	841.565	Yellow; Blue; Violet; Green; Red	674901.2235	913678.9329	3.21E+07	3.01E+07	5.49E+07
562	1687.7784	Yellow; Blue; Violet; Green; Red	2.75E+07	6.51E+07	1.44E+08	7.04E+07	5.85E+07
563	846.6576	Yellow; Blue; Violet; Green; Red	9388533.274	5102693.189	9.37E+07	3521174.922	30514.77268
564	1692.7333	Yellow; Blue; Violet; Green; Red	1.90E+07	5.09E+07	1.03E+08	5.28E+07	4.01E+07
565	1695.7365	Yellow; Blue; Violet; Green; Red	888942.0407	7494884.781	7280519.919	2879985.286	374955.3672
566	1697.6867	Yellow; Blue; Violet; Green; Red	8610322.225	1.65E+07	2.02E+07	1.66E+07	1.11E+07
567	853.5537	Yellow; Blue; Violet; Green; Red	359503.371	6736697.475	2.59E+07	9471183.359	1553796.367
568	860.4683	Yellow; Blue; Violet; Green; Red	2391309.945	2.65E+07	6.12E+07	3.09E+07	1.39E+07
569	1729.789	Yellow; Blue; Violet; Green; Red	9511877.364	7.01E+07	9.27E+07	3.19E+07	9730632.548

570	1734.7437	Yellow; Blue; Violet; Green; Red	8131360.059	5.17E+07	6.82E+07	2.05E+07	7732131.172
571	1739.6972	Yellow; Blue; Violet; Green; Red	3023408.771	1.62E+07	1.56E+07	9215273.847	2079598.407
572	870.5801	Yellow; Blue; Violet; Green; Red	1257359.015	1.68E+07	8.25E+07	2.87E+07	3660476.854
573	875.5355	Yellow; Blue; Violet; Green; Red	1973746.761	1.73E+07	8.69E+07	3.11E+07	6202384.539
574	878.4021	Yellow; Blue; Violet; Green; Red	6311546.994	1.40E+07	1.52E+07	5113970.779	903530.7335
575	878.4021	Yellow; Blue; Violet; Green; Red	9216205.3	8312007.647	1.54E+07	5066771.542	3966505.256
576	879.3863	Yellow; Blue; Violet; Green; Red	7799454.212	1.13E+07	8212267.305	7621218.565	6298962.022
577	883.6786	Yellow; Blue; Violet; Green; Red	1.34E+07	2315382.087	8320683.414	345599.9766	12111.8448
578	1773.8157	Yellow; Blue; Violet; Green; Red	3.26E+07	5.02E+07	1.15E+08	6.13E+07	3.90E+07
579	887.5682	Yellow; Blue; Violet; Green; Red	4.45E+07	1.81E+07	1.88E+07	4532545.972	2153551.963
580	1778.7703	Yellow; Blue; Violet; Green; Red	2.09E+07	3.75E+07	8.17E+07	4.17E+07	2.73E+07
581	1783.7234	Yellow; Blue; Violet; Green; Red	8978820.63	1.17E+07	1.64E+07	1.68E+07	1.13E+07
582	893.7207	Yellow; Blue; Violet; Green; Red	1.56E+07	1.95E+07	3.08E+07	3922970.961	9021366.861
583	896.4131	Yellow; Blue; Violet; Green; Red	4.93E+07	6.36E+07	8.54E+07	3.94E+07	2.93E+07
584	900.384	Yellow; Blue; Violet; Green; Red	6588529.273	1.36E+07	1.64E+07	4947019.826	704266.2438
585	901.3682	Yellow; Blue; Violet; Green; Red	6.10E+07	7.45E+07	1.03E+08	4.29E+07	3.24E+07
586	1815.8261	Yellow; Blue; Violet; Green; Red	8041683.858	5.09E+07	5.93E+07	2.01E+07	5999198.999
587	1820.7806	Yellow; Blue; Violet; Green; Red	8225091.653	3.70E+07	4.21E+07	1.27E+07	4327013.924
588	1825.734	Yellow; Blue; Violet; Green; Red	2269870.202	1.23E+07	1.10E+07	6755151.136	1073957.462

589	1841.8417	Yellow; Blue; Violet; Green; Red	1046059.931	4925409.273	3268255.557	1.79E+07	4.28E+07
590	1846.7961	Yellow; Blue; Violet; Green; Red	707550.8689	4344491.814	2095982.098	1.41E+07	2.47E+07
591	924.613	Yellow; Blue; Violet; Green; Red	232077.2887	2142970.605	2503230.736	3.69E+07	1.68E+07
592	928.6875	Yellow; Blue; Violet; Green; Red	813034.6924	53439.80643	1.97E+07	160440.8668	0
593	1859.8528	Yellow; Blue; Violet; Green; Red	1.85E+07	2.45E+07	5.73E+07	3.76E+07	2.19E+07
594	1864.8072	Yellow; Blue; Violet; Green; Red	1.62E+07	1.93E+07	3.81E+07	2.27E+07	1.16E+07
595	944.642	Yellow; Blue; Violet; Red	0	275213.9771	87008.4829	1.59E+07	4459785.826
596	947.3982	Yellow; Violet	0	1042987.917	25167.07523	0	0
597	949.5462	Yellow; Blue; Violet; Green; Red	1.52E+07	282777.491	2199406.527	8476.015871	4921.867732
598	1901.8624	Yellow; Blue; Violet; Green; Red	6207177.332	2.17E+07	3.62E+07	1.18E+07	2978537.948
599	1906.8166	Yellow; Blue; Violet; Green; Red	4465557.534	1.59E+07	2.35E+07	1.26E+07	2258179.113
600	1915.8774	Yellow; Blue; Violet; Green; Red	1358631.414	891984.4588	1.77E+07	719195.5834	145119.1476
601	1920.8322	Yellow; Blue; Violet; Green; Red	803470.9068	560086.7382	9512892.046	426252.4577	128143.7405
602	961.7552	Yellow; Blue; Violet; Green; Red	2594056.503	1.37E+07	1.76E+07	4.34E+07	3.41E+07
603	963.596	Yellow; Blue; Violet; Green; Red	1.90E+07	8265534.135	2906815.185	7439872.522	7508749.959
604	964.4388	Yellow; Blue; Violet; Green; Red	1.09E+07	1.80E+07	2.93E+07	8656283.403	7382026.201
605	965.4232	Yellow; Blue; Violet; Green; Red	6952141.938	9191536.116	1.17E+07	7015296.757	6262212.82
606	965.5411	Yellow; Violet; Green; Red	6846923.246	206468.0427	2387465.653	2852.960812	0
607	966.6235	Yellow; Blue; Violet; Red	0	1228722.921	548476.5991	5.68E+07	1.01E+07

608	966.6238	Yellow; Blue; Violet; Green; Red	9102.480073	670952.2714	417081.3594	2.70E+07	1.90E+07
609	969.394	Yellow; Blue; Violet; Green; Red	8635500.988	1.39E+07	1.92E+07	5549875.051	5086866.746
610	971.6589	Yellow; Blue; Violet; Red	0	2377750.115	10188.23271	131107.1045	3712.868973
611	1945.8883	Yellow; Blue; Violet; Green; Red	1.23E+07	8342858.004	2.14E+07	1.56E+07	8336563.24
612	982.4499	Yellow; Blue; Violet; Green; Red	3.30E+07	5.57E+07	8.51E+07	3.74E+07	3.26E+07
613	983.737	Yellow; Blue; Violet; Green; Red	3420094.416	1.46E+07	1.33E+07	5.63E+07	4.20E+07
614	985.5771	Yellow; Blue; Violet; Green; Red	1.78E+07	9043176.52	4054816.82	7691859.12	6656241.883
615	986.6514	Yellow; Blue; Violet; Green; Red	3.40E+07	5981921.545	3111105.033	1.36E+07	1.31E+07
616	987.4049	Yellow; Blue; Violet; Green; Red	3.79E+07	6.16E+07	9.77E+07	4.04E+07	3.44E+07
617	990.7035	Violet	0	0	8.50E+07	0	0
618	995.6583	Yellow; Violet; Green	2855.572453	5518.864312	7.35E+07	0	0
619	997.6713	Yellow; Blue; Violet; Green; Red	1.44E+07	8163563.183	2.74E+07	8189019.629	1890256.275
620	997.7496	Yellow; Blue; Violet; Green; Red	109878.4772	4.25E+07	7.06E+07	4.66E+07	2293416.395
621	1005.6335	Yellow; Blue; Violet; Green; Red	6706.701628	26845.68545	1.48E+07	4.81E+07	9.09E+07
622	1011.687	Yellow; Blue; Violet; Green; Red	2.08E+07	9739109.509	2.54E+07	1.18E+07	2216319.436
623	1014.6826	Yellow; Blue; Violet; Green; Red	2.30E+07	2506195	2239601.97	4905697.993	4874771.654
624	1017.64	Yellow; Blue; Violet; Green; Red	24583.38352	21573.39888	1.88E+07	11727.15197	16771.42063
625	1019.7319	Yellow; Blue; Violet; Green; Red	17127.40929	1.23E+07	1.61E+07	1.12E+07	697701.5705
626	2045.9412	Yellow; Blue; Violet; Green; Red	319276.2733	1688453.321	1723542.293	1.03E+07	1.77E+07
627	1023.7632	Yellow; Blue; Violet; Green; Red	543333.0623	9.93E+07	1.91E+08	1.22E+08	8313102.608

628	1030.7558	Yellow; Blue; Violet; Green; Red	60790.07096	2.40E+07	2.53E+07	1.15E+07	194202.4746
629	1042.8445	Yellow; Violet; Green; Red	1583555.03	1583690.305	5.08E+07	5898.749945	0
630	1044.7716	Yellow; Blue; Violet; Green; Red	75168.49504	5.18E+07	1.36E+08	3.83E+07	368859.434
631	1044.8082	Yellow; Blue; Violet; Green; Red	4488911.262	1.20E+07	3.19E+07	9920363.714	178354.5009
632	1044.8599	Yellow; Violet; Green; Red	1265546.99	2853587.226	5.88E+07	3797.973816	0
633	1049.7629	Yellow; Blue; Violet; Green; Red	1.43E+07	2.20E+07	7.12E+07	2.10E+07	573449.8034
634	1050.4758	Yellow; Blue; Violet; Green; Red	8841202.748	1.54E+07	1.71E+07	7809781.233	8913864.464
635	1051.4604	Yellow; Blue; Violet; Green; Red	4663439.652	7777303.479	8684043.992	6319077.541	6452481.304
636	1055.4311	Yellow; Blue; Violet; Green; Red	8401757.919	9088136.293	1.44E+07	5109503.005	6018349.423
637	1055.7744	Yellow; Violet; Green	94369.43159	2216.627994	2.34E+07	0	0
638	1060.8034	Yellow; Blue; Violet; Green; Red	1.16E+07	1.97E+08	4.33E+08	7.86E+07	2000834.496
639	1060.8036	Yellow; Blue; Violet; Green; Red	6738613.636	4.67E+07	8.61E+07	561240.5864	1339428.158
640	1065.7576	Yellow; Blue; Violet; Green; Red	1.13E+07	5.12E+07	9.98E+07	754173.5701	5261.709964
641	1065.7577	Yellow; Blue; Violet; Green; Red	1.29E+07	1.75E+08	3.75E+08	7.70E+07	1465893.898
642	1068.4866	Yellow; Blue; Violet; Green; Red	2.09E+07	5.02E+07	8.31E+07	3.74E+07	3.90E+07
643	1073.4416	Yellow; Blue; Violet; Green; Red	2.08E+07	4.53E+07	8.34E+07	3.54E+07	3.47E+07
644	1074.782	Yellow; Blue; Violet; Green; Red	6816885.999	3286357.725	8.97E+07	1.28E+07	1346170.368
645	1081.7312	Yellow; Blue; Violet; Green; Red	1607132.871	1.88E+07	3.11E+07	9582604.303	106032.8469
646	1084.8712	Yellow; Blue; Violet; Green; Red	9178419.51	2750076.328	4.43E+07	7357855.707	23753.40171

647	1086.7817	Yellow; Blue; Violet; Green; Red	28797.1403	2.36E+07	6.53E+07	1.80E+07	438961.3457
648	1105.931	Yellow; Violet; Green	284878.2935	1.19E+08	5483241.181	0	0
649	1105.931	Yellow; Violet; Green	5107.350506	2.68E+07	483331.5346	0	0
650	1106.6826	Yellow; Blue; Violet; Green; Red	1145706.049	7846560.472	2.55E+07	1.00E+07	3906020.853
651	1106.7453	Yellow; Blue; Violet; Green; Red	2.38E+07	2.51E+07	2.38E+07	1.65E+07	1.81E+07
652	1108.7636	Yellow; Blue; Violet; Green; Red	106992.866	4.27E+07	1.30E+08	3.03E+07	852584.2468
653	1110.4966	Yellow; Blue; Violet; Green; Red	3707108.02	7111668.403	1.30E+07	6409202.783	3337988.111
654	1115.452	Yellow; Blue; Violet; Green; Red	2848712.201	5215030.154	1.06E+07	5540766.959	2815950.521
655	1116.7928	Yellow; Blue; Violet; Green; Red	697680.4803	692293.3659	1.78E+07	4236147.415	238375.4707
656	1136.5125	Yellow; Blue; Violet; Green; Red	8329328.018	1.12E+07	9649801.744	5600149.232	8194232.315
657	1138.7741	Yellow; Blue; Violet; Green; Red	2402744.557	2467374.053	6.95E+07	1.06E+07	716374.7911
658	1142.8448	Yellow; Blue; Violet; Green; Red	814545.9287	698658.0156	9.04E+07	6633648.618	184167.6665
659	1154.5238	Yellow; Blue; Violet; Green; Red	1.78E+07	4.30E+07	7.43E+07	3.32E+07	3.83E+07
660	1158.8395	Yellow; Blue; Violet; Green; Red	48078.2113	564582.0838	1.97E+07	1857413.75	23148.36208
661	1158.8397	Yellow; Blue; Violet; Green; Red	2922231.408	2990337.221	9.17E+07	5241633.38	29954.17188
662	1159.4788	Yellow; Blue; Violet; Green; Red	1.37E+07	3.86E+07	6.83E+07	3.16E+07	3.78E+07
663	1172.8556	Yellow; Blue; Violet; Green; Red	8194314.04	1.03E+07	6.47E+08	3.04E+07	2096553.518
664	1172.8558	Yellow; Blue; Violet; Green; Red	8194314.04	7161360.704	7.18E+08	3.93E+07	2096553.518
665	1174.7828	Yellow; Blue; Violet; Green; Red	260521.9562	1.06E+07	9045815.334	1.89E+07	2.40E+07

666	1194.8372	Yellow; Blue; Violet; Green; Red	158472.9099	439574.5471	2.75E+07	1380562.987	35198.98555
667	1200.8529	Yellow; Blue; Violet; Green; Red	118795.5647	582008.098	9327268.012	76985.27936	5801.006333
668	1202.8668	Yellow; Blue; Violet; Green; Red	1.22E+07	5505086.36	2.73E+07	77590.37243	3097.594512
669	1204.8819	Yellow; Blue; Violet; Green; Red	26800.80918	1.07E+07	1.03E+07	2445029.11	68223.79878
670	1206.8372	Yellow; Blue; Violet; Green; Red	195876.3737	348278.6704	3.07E+07	1675625.04	56872.4789
671	1208.7676	Yellow; Blue; Violet; Green; Red	307807.9401	1.16E+07	9306763.48	1.81E+07	1.88E+07
672	1214.8663	Yellow; Blue; Violet; Green; Red	2928327.131	1919369.257	2.64E+08	1.30E+07	944156.6694
673	1222.5493	Yellow; Blue; Violet; Green; Red	1.12E+07	2.61E+07	2.24E+07	8673182.098	3.24E+07
674	1222.8313	Yellow; Blue; Violet; Green; Red	1408309.021	2209191.886	1.44E+07	1506228.454	234296.1571
675	1222.8318	Yellow; Blue; Violet; Green; Red	1209101.688	1914554.044	3.29E+07	525636.5045	20405.74823
676	1227.5047	Yellow; Blue; Violet; Green; Red	7933124.729	1.56E+07	1.61E+07	5604282.939	2.47E+07
677	1229.811	Yellow; Blue; Violet; Green; Red	9124906.583	5511636.611	397691.3292	8504037.348	1.49E+07
678	1236.8475	Yellow; Blue; Violet; Green; Red	5112282.559	4067877.459	3.97E+08	1.60E+07	1275342.304
679	1240.5605	Yellow; Blue; Violet; Green; Red	1.09E+07	3.28E+07	5.51E+07	2.50E+07	4.46E+07
680	1245.5155	Yellow; Blue; Violet; Green; Red	1.43E+07	3.17E+07	5.53E+07	2.14E+07	4.27E+07
681	1261.7976	Yellow; Blue; Violet; Green; Red	7450255.335	3809482.184	9537712.708	3663041.875	436137.6514
682	1270.9283	Yellow; Blue; Violet; Green; Red	100438.1203	738593.1915	4.82E+07	842310.8774	27603.38135
683	1295.0078	Yellow; Violet; Green; Red	15035.5687	56136.64172	1.44E+08	20416.68447	0
684	1326.5975	Yellow; Blue; Violet; Green; Red	1.49E+07	2.22E+07	4.32E+07	2.72E+07	2.59E+07

685	1331.5526	Yellow; Blue; Violet; Green; Red	1.22E+07	2.01E+07	4.00E+07	2.44E+07	2.61E+07
686	1334.9214	Yellow; Blue; Violet; Green; Red	323078.0599	2879018.376	5.28E+07	4951704.541	27983.55701
687	1338.9038	Yellow; Violet; Green; Red	573172.565	5000615.135	4.08E+07	248691.2403	0
688	1343.8584	Yellow; Violet; Green; Red	3368854.041	1.00E+07	1.03E+07	94078.23049	0
689	1343.8587	Yellow; Blue; Violet; Green; Red	1708993.785	1.20E+07	7.59E+07	873114.7533	8281.19545
690	1344.9141	Yellow; Blue; Violet; Green; Red	1589947.033	2631675.401	3.50E+07	39088.17411	4613.210347
691	1360.8974	Yellow; Violet; Green; Red	9822632.39	3564667.511	410549.246	1594.417056	0
692	1365.853	Yellow; Violet; Green; Red	1.97E+07	8740627.116	2009846.03	99926.83479	0
693	1378.4446	Yellow; Blue; Violet; Red	0	1203886.466	458869.2606	8505918.822	6525222.179
694	1390.9711	Yellow; Blue; Violet; Green; Red	4068182.534	2.57E+07	3.14E+07	1.33E+07	62426.02945
695	1395.9259	Yellow; Blue; Violet; Green; Red	1.24E+07	9.20E+07	1.16E+08	3.24E+07	982337.0317
696	1395.9264	Yellow; Blue; Violet; Green; Red	1.16E+07	7.00E+07	8.56E+07	3.05E+07	882942.6673
697	1406.9643	Yellow; Violet; Green; Red	7622334.383	2.66E+07	3.67E+07	136364.6187	0
698	1406.9649	Yellow; Violet; Green; Red	535399.0769	8706583.511	9.02E+07	343822.9464	0
699	1411.9194	Yellow; Violet; Green; Red	844751.6098	1.59E+07	1.13E+08	633903.5889	0
700	1411.9196	Yellow; Violet; Green; Red	1.20E+07	5.82E+07	7.25E+07	708798.6445	0
701	1412.6329	Yellow; Blue ;Violet; Green; Red	1.12E+07	2.71E+07	5.13E+07	2.32E+07	2.38E+07
702	1417.5878	Yellow; Blue; Violet; Green; Red	1.05E+07	2.95E+07	5.24E+07	3.04E+07	3.44E+07
703	1418.9648	Yellow;Violet	0	11517.74736	5017524.827	0	0

704	1425.8975	Yellow; Violet; Green; Red	28127.00486	1610520.542	6649716.253	105073.3988	0
705	1436.9752	Violet; Green; Red	1224.973297	0	9733777.269	12316.74315	0
706	1441.9302	Yellow; Violet; Green; Red	7173.075539	1371.161949	1.77E+07	29480.06985	0
707	1454.643	Yellow; Blue; Violet; Green; Red	2327673.128	8106146.17	1.07E+07	6743608.142	3018881.307
708	1459.5983	Yellow; Blue; Violet; Green; Red	2054614.822	7462272.264	1.12E+07	5925506.801	2738182.63
709	1465.0067	Yellow; Blue; Violet; Green; Red	1.73E+07	1.04E+08	1.42E+08	2.71E+07	272598.9489
710	1465.0067	Yellow; Blue; Violet; Green; Red	1.74E+07	1.34E+08	1.88E+08	3.34E+07	282401.5406
711	1479.0221	Yellow; Blue; Violet; Green; Red	1.17E+07	9100650.813	3.25E+07	4234813.467	93394.87696
712	1480.659	Yellow; Blue; Violet; Green; Red	3204439.798	9990113.749	1.36E+07	1.12E+07	9837426.765
713	1481.001	Yellow; Violet; Green; Red	828781.0148	5160526.273	8.04E+07	180761.141	0
714	1481.0014	Yellow; Violet; Green; Red	1.10E+07	3.68E+07	4.08E+07	232033.4556	0
715	1485.614	Yellow; Blue; Violet; Green; Red	3550707.057	8967539.95	1.33E+07	6160498.202	5320833.908
716	1486.9882	Yellow; Blue; Violet; Green; Red	1.55E+07	1.07E+08	1.46E+08	5.49E+07	481223.9732
717	1486.9883	Yellow; Blue; Violet; Green; Red	1.55E+07	1.60E+08	1.37E+08	2.84E+07	619648.7137
718	1495.017	Yellow; Violet; Green; Red	1317551.123	1.13E+07	2.10E+07	36313.09756	0
719	1495.017	Yellow; Violet; Green; Red	348495.1448	2900368.915	3.99E+07	62828.42287	0
720	1498.6695	Yellow; Blue; Violet; Green; Red	8525800.529	1.57E+07	2.96E+07	1.31E+07	1.20E+07
721	1502.9827	Yellow ;Violet; Green; Red	125507.805	5042952.75	2.48E+07	93243.79499	0
722	1503.6245	Yellow; Blue; Violet; Green; Red	6585586.361	1.59E+07	2.95E+07	1.03E+07	1.44E+07

723	1524.1492	Yellow; Blue; Violet; Green; Red	35390.04919	3.58E+07	7.24E+07	4.74E+07	1675765.692
724	1540.6802	Yellow; Blue; Violet; Green; Red	2872293.55	1.10E+07	1.37E+07	8387993.624	3951568.957
725	1545.6351	Yellow; Blue; Violet; Green; Red	2590150.21	1.04E+07	1.32E+07	7199527.839	3250440.31
726	1584.7065	Yellow; Blue; Violet; Green; Red	6520391.07	1.47E+07	2.82E+07	1.15E+07	1.40E+07
727	1589.6611	Yellow; Blue; Violet; Green; Red	6201229.193	1.55E+07	3.13E+07	1.13E+07	1.41E+07
728	1619.4814	Yellow; Blue; Violet; Green; Red	2830313.603	5.62E+07	4.68E+07	8.08E+07	7.86E+07
729	1626.7169	Yellow; Blue; Violet; Green; Red	2433095.013	1.19E+07	1.50E+07	7319221.963	2246491.487
730	1631.6717	Yellow; Blue; Violet; Green; Red	2445171.982	1.08E+07	1.76E+07	6948378.073	2309600.809
731	1670.744	Yellow; Blue; Violet; Green; Red	6552833.446	1.14E+07	2.63E+07	1.25E+07	8124646.26
732	1675.6986	Yellow; Blue; Violet; Green; Red	4811265.611	1.53E+07	3.55E+07	1.53E+07	1.12E+07
733	1712.7542	Yellow; Blue; Violet; Green; Red	1675717.978	8921653.24	1.33E+07	5577356.419	1034012.418
734	1717.7091	Yellow; Blue; Violet; Green; Red	1927720.001	1.15E+07	1.77E+07	6025300.927	1104004.026
735	1761.7353	Yellow; Blue; Violet; Green; Red	5100111.923	7723025.336	1.59E+07	1.01E+07	6992105.775
736	1798.7911	Yellow; Blue; Violet; Green; Red	759924.6001	4385129.829	5512560.867	2729233.786	344952.6059
737	1803.7458	Yellow; Blue; Violet; Green; Red	1033220.022	6131925.435	7166402.368	3012205.882	473864.2549

Table S2.- Dataset used for the construction of the molecular networks with Cytoscape